AD-A182 129 ANALYSIS AND EXPERIMENTAL IMPLEMENTATION OF OPTICAL BEAMFORMERS(U) NAVAL RESEARCH LAB WASHINGTON DC R D GRIFFIN ET AL. 20 MAY 87 NRL-MR-5995 1/1

UNCLASSIFIED F/G 9/5 NL

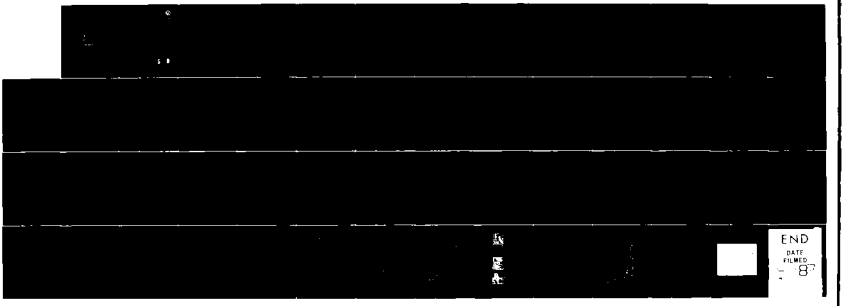

END
DATE FILMED
8-87

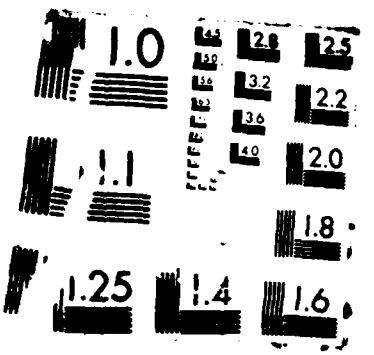
1.0
1.1
1.25
1.4
1.6
1.8
2.0
2.2
2.5
2.8
3.2
3.6
4.0

Naval Research Laboratory
Washington, DC 20375-5000

NRL Memorandum Report 5995

Analysis and Experimental Implementation of Optical Beamformers

RICHARD D. GRIFFIN, PETER B. ROLSMA AND JOHN N. LEE

Applied Optics Branch
Optical Sciences Division

May 20, 1987

87

SECURITY CLASSIFICATION OF THIS PAGE A182129

REPORT DOCUMENTATION PAGE

1a. REPORT SECURITY CLASSIFICATION UNCLASSIFIED	1b. RESTRICTIVE MARKINGS
2a. SECURITY CLASSIFICATION AUTHORITY	3. DISTRIBUTION/AVAILABILITY OF REPORT Approved for public release; distribution unlimited.
2b. DECLASSIFICATION/DOWNGRADING SCHEDULE	
4. PERFORMING ORGANIZATION REPORT NUMBER(S) NRL Memorandum Report 5995	5. MONITORING ORGANIZATION REPORT NUMBER(S)
6a. NAME OF PERFORMING ORGANIZATION Naval Research Laboratory 6b. OFFICE SYMBOL (If applicable) Code 6530	7a. NAME OF MONITORING ORGANIZATION
6c. ADDRESS (City, State, and ZIP Code) Washington, DC 20375-5000	7b. ADDRESS (City, State, and ZIP Code)
8a. NAME OF FUNDING/SPONSORING ORGANIZATION Office of Naval Technology 8b. OFFICE SYMBOL (If applicable)	9. PROCUREMENT INSTRUMENT IDENTIFICATION NUMBER
8c. ADDRESS (City, State, and ZIP Code) Arlington, VA 22217-5000	10. SOURCE OF FUNDING NUMBERS PROGRAM ELEMENT NO. PE62314 / PROJECT NO. RJ14C37 / TASK NO. / WORK UNIT ACCESSION NO. DN380-062
11. TITLE (Include Security Classification) Analysis and Experimental Implementation of Optical Beamformers	
12. PERSONAL AUTHOR(S) Griffin, Richard D., Rolsma, Peter B., and Lee, John N.	
13a. TYPE OF REPORT Memorandum 13b. TIME COVERED FROM _____ TO _____ 14. DATE OF REPORT (Year, Month, Day) 1987 May 20 15. PAGE COUNT 54	
16. SUPPLEMENTARY NOTATION	
17. COSATI CODES FIELD / GROUP / SUB-GROUP	18. SUBJECT TERMS (Continue on reverse if necessary and identify by block number) Beamformer Optics Sonar

19. ABSTRACT (Continue on reverse if necessary and identify by block number)

Most modern beamformers are implemented on a digital computer. Some proposed sonar systems will tax the ability of a conventional beamformer design to supply the needed beam samples at an acceptable rate. In addition, there exist applications which require low power consumption and small size: present-day systems are only marginally acceptable. This report examines the potential for analog optical beamforming systems to meet the proposed requirements.

The report begins with a discussion of the various beamforming algorithms and their calculational complexity; a list of the strengths and weaknesses of digital implementations is also included. Various general algorithms for time- and frequency-domain optical beamforming are then described. Special emphasis is placed on the importance of designing efficient interfaces between analog optical and electronic systems and digital systems. Details of three implementations of optical beamformers are presented in the next chapter: cross-bar and partial-sum time-domain beamformers, and a vector-matrix frequency-domain beamformer.

Continues

20. DISTRIBUTION/AVAILABILITY OF ABSTRACT ☒ UNCLASSIFIED/UNLIMITED ☐ SAME AS RPT. ☐ DTIC USERS	21. ABSTRACT SECURITY CLASSIFICATION UNCLASSIFIED
22a. NAME OF RESPONSIBLE INDIVIDUAL Richard D. Griffin	22b. TELEPHONE (Include Area Code) 202-767-5630 22c. OFFICE SYMBOL Code 6530

DD FORM 1473, 84 MAR 83 APR edition may be used until exhausted. All other editions are obsolete. SECURITY CLASSIFICATION OF THIS PAGE

19. ABSTRACT (Continued)

Without further research it is not possible to determine the maximum practical capability of an optical beamformer, but frequency domain optical beamforming systems look promising for systems requiring large numbers of beams. The experimental optical vector-matrix processor has been designed, constructed, and configured to perform frequency domain beamforming at a rate of 2×10^9 8-bit multiplies/sec. It also is likely that optical beamformers can meet the low power and size requirements in certain applications such as on-board processing for sonobuoys employing hydrophone arrays: an architecture has been developed with potential power consumption of <20mW. Early architectures were implemented using commercial liquid-crystal display devices but their response times proved inadequate. The more promising architecture uses fiberoptic couplers and a photodetector array/CCD MUX and is currently in the breadboarding stage of development.

CONTENTS

I. INTRODUCTION 1

II. CONVENTIONAL BEAMFORMING 3

A. Beamforming Fundamentals 3
B. Time-Domain Beamforming 6
C. Frequency-Domain Beamforming 8
D. General Considerations and Digital Implementations 9

III. OPTICAL BEAMFORMING 12

A. Introduction 12
B. Time-Domain Optical Beamforming 14
C. Frequency-Domain Optical Beamforming 18
D. Interfacing 19

IV. OPTICAL BEAMFORMING: IMPLEMENTATION DETAILS AND EXPERIMENTAL RESULTS 20

A. Implementation of an Optical Cross-Bar Beamformer 20
B. Implementation of a Partial-Sum Beamformer 23
C. Implementation of a Vector-Matrix Frequency-Domain Beamformer 24

V. SUMMARY AND CONCLUSIONS 26

REFERENCES 29

APPENDIX—Calculation of Half-Power Beamwidths 31

ANALYSIS AND EXPERIMENTAL IMPLEMENTATION OF OPTICAL BEAMFORMERS

I. INTRODUCTION

Tremendous sensitivity is required in sonar systems designed to locate and track quiet targets at great distances. In order to improve the detection probability in underwater acoustic surveillance, the signals from individual sensors of a hydrophone array are coherently summed according to various schemes in a process termed beamforming or beamsteering. The resulting array spatial response or sensitivity pattern usually has one main lobe and several smaller sidelobes, thus discriminating against localized sources and achieving S/N gain against isotropic (uncorrelated) noise. The nominal beamwidth of the array is proportional to the ratio of wavelength to array-aperture dimension; the gain of the array is generally proportional to the number of sensors. Beamforming is just one step in what is often a complex sequence of signal processing operations. These operations may provide for additional S/N improvement, target location, identification, and tracking.

The resources that can be allocated to sonar signal processing are limited; this implies constraints on the design of a beamforming system. These constraints may be divided into two groups: i) those arising from the application, and ii) those imposed by the available devices. For example, remote platforms dictate a particularly difficult set of constraints: the data must be transmitted to a receiving station (airplane, satellite, etc.), and this operation consumes most of the available power; in turn the available power is limited by the energy storage technology. These constraints have forced designers of sonobuoys to limit the signal processing to rudimentary forms. The latter group of constraints thus has a profound effect on the first: a new technology often creates new applications.

Early beamforming systems were analog and operated in the time domain via delay lines. The growth of digital technology afforded new flexibility and improved signal processing techniques, which led to higher detection probabilities. Some future systems will probably incorporate large numbers of sensors

Manuscript approved March 4, 1987

for increased gain, but current digital technology will have difficulty with the increased processing loads. Before better systems can be built, significant improvements in digital signal processing algorithms and hardware must be made or a new technology must be developed.

A recent development in detector technology is the fiber optic hydrophone[1]. This development, along with the need for low-power, compact hardware, and the projected increase in processing loads have led some researchers to explore the use of optical techniques in beamforming and other sonar signal processing operations[2]. In this report we describe several optical beamformer architectures developed and studied at NRL.

In the next chapter we review conventional beamforming. The mathematical foundation of time-domain beamforming is described first, as it provides a physical model which one can readily understand. The processing requirements for various forms of time-domain beamforming are then stated. In the following section frequency-domain techniques are discussed, and the fundamental equation is derived by taking the Fourier transform of the basic time-domain beamforming equation. A discussion of the general requirements that a beamforming system must satisfy is presented in the last section. Included is a presentation of the advantages and disadvantages of digital beamforming.

The rationale for building an optical analog beamformer begins the following chapter; we then describe a frequency-domain and three time-domain architectures. Each type is best suited to a particular set of hardware. Experimental versions of three of the architectures are described in the next chapter to show how the effectiveness of a particular architecture is determined by the available technology. In all cases it is clear that the quality of the interfaces between the optical system and the input and output systems is of critical importance in the attainable performance of a particular implementation.

The case for further study of the application of opto-electronic technology to beamforming is made by pointing out the advantages accruing to this technology in applications which require speed, low power, or compactness more than precision.

II. CONVENTIONAL BEAMFORMING

Beamforming is a process of combining the outputs of an array of sensors in such a way as to enhance the measured amplitude of a spatially coherent wavefront relative to ambient background noise and spatially localized interfering sources. This is commonly achieved by properly time-delaying, weighting and summing the sensor outputs as described in Section II-A. The time delays cause the array to "look" in the proper direction; weighting modifies the angular response pattern of the array to minimize the effect of sidelobes.

A. Beamforming Fundamentals

Suppose there is an array of N sensors of known locations $\mathbf{X}_n$ in a coordinate system (x,y,z). Let the output signal of a sensor at the origin be $e(t)$. The response of a sensor at $\mathbf{X}_n$ to a planar wavefront propagating from a direction K (propagation vector -K) is given by

$$e_n(t) = e[t + (\mathbf{X}_n \cdot \mathbf{K})/c] \ , \tag{2-1}$$

where c is the wavefront propagation speed. By delaying the sensor outputs by an amount $(\mathbf{X}_n \cdot \mathbf{B}_m)/c$ and summing we obtain the beamforming equation

$$b_m(t) = \sum_{n=0}^{N-1} e_n\left[t - \frac{\mathbf{X}_n \cdot \mathbf{B}_m}{c}\right]$$

$$= \sum_{n=0}^{N-1} e\left[t - \frac{\mathbf{X}_n \cdot (\mathbf{B}_m - \mathbf{K})}{c}\right] \ , \tag{2-2}$$

where $\mathbf{B}_m$ is the m-th beamsteering or look-direction vector. If $\mathbf{B}_m = \mathbf{K}$, then the amplitude of the beamformed output is N times that of the signal at the origin. For uncorrelated noise, this implies an enhancement of N in signal-to-noise ratio[3,4]. This operation also discriminates against off-axis, localized noise sources. The width of the main lobe of the array response pattern is determined by the projected aperture of the array in the beamsteering direction and on the particular planar slice chosen. For a one dimensional array, the nominal beamwidth is λ/L rad, where λ is the wavelength of interest and L is the width of the projected aperture. Although Eq. (2-2) is valid for arbitrary sensor locations, throughout the remainder of the report we will apply it to a linear array of sensors.

Let there be a source of planar, sinusoidal traveling waves of angular frequency $\omega = 2\pi f$ located a large distance from a linear array of sensors uniformly spaced a distance d apart, and let the wavefronts make an angle θ_0 with respect to a perpendicular to the array axis, as shown in Fig. 1. The propagation direction is then given by

$$-\mathbf{K} = -(\sin\theta_0\hat{\mathbf{x}} + \cos\theta_0\hat{\mathbf{y}}) \ , \tag{2-3}$$

and the time dependence of the signal at a sensor is given by

$$e(t) = 2E_0\cos(\omega t) \ , \tag{2-4}$$

where E_0 is a constant. The result of applying Eq. (2-2) is

$$b_m(t) = E_0\, e^{j\omega t} \sum_n \exp[-j\omega(\tau_{nm} - \frac{nd}{c}\sin\theta_0)] + \text{c.c.} \ , \tag{2-5}$$

where

$$\tau_{nm} = \mathbf{X}_n \cdot \mathbf{B}_m = \frac{nd}{c}\sin\theta_m \ , \tag{2-6}$$

and θ_m is the m-th look direction. The amplitude of Eq. (2-5) is given by

$$|b_m(t)| = 2NE_0\cos[\omega t + (N-1)\alpha(\theta_m)]\ g(\theta_m) \ , \tag{2-7}$$

where

$$g(\theta) = \frac{\sin(N\alpha)}{N\sin\alpha} \ , \tag{2-8}$$

and

$$\alpha(\theta) = \frac{1}{2c}\omega d(\sin\theta - \sin\theta_0) \ . \tag{2-9}$$

The beam response pattern, $g(\theta)$, is illustrated in Fig. 2 as a function of θ for $\theta_0 = -30$ deg. If $\theta = \theta_0$, which is the maximum response axis (MRA), we see that

$$b(t) = Ne(t) \ .$$

The half-power width is found by solving for $\theta_{\frac{1}{2}}$ which satisfies

$$g(\theta_{\frac{1}{2}}) = \frac{g(\theta_0)}{\sqrt{2}} = \frac{1}{\sqrt{2}} \ , \tag{2-10}$$

and is given approximately by

$$\sin\theta_{\frac{1}{2}} \approx \sin\theta_0 \pm 0.443\,\frac{c}{Nfd} \ . \tag{2-11}$$

Thus the beamwidth in $\sin\theta$-space is given approximately by

$$\delta(\sin\theta_{\frac{1}{2}}) \approx 0.886\,\frac{c}{Nfd} \ . \tag{2-12}$$

To span the azimuthal domain,

$$N_B \approx \frac{Nfd}{0.443c} \tag{2-13}$$

beams are required. For $d = \lambda/2$, $N_B \approx (1.13)N$. A Pascal computer program which solves for the half-power maximum response axes is given in the Appendix along with the results for several values of N.

If we modify Eq. (2-5) by weighting the sensor values with coefficients a_n, then

$$b_m(t) = E_0 \, e^{j\omega t} \sum_n a_n e^{-j2\pi nd(\beta-\beta_0)} + c.c. \tag{2-14}$$

where

$$\beta = \frac{f \sin\theta}{c} \tag{2-15}$$

and

$$\beta_0 = \frac{f \sin\theta_0}{c} \, . \tag{2-16}$$

Notice that the summation term looks like a discrete Fourier transform (DFT) of the a_n evaluated at the spatial frequency $\beta - \beta_0$. Thus, the "windowing" techniques of Fourier transform theory[5] may be used to reduce the sidelobe levels at the expense of a slightly increased beamwidth. Adjustment of the a_n in real time is the basis for adaptive beamforming[6].

With the addition of the weighting coefficients, Eq. (2-5) may be rewritten as

$$b_m(t) = \sum_{n=0}^{N-1} a_n e_n(t-\tau_{nm}) \, . \tag{2-17}$$

This equation describes the basic time-domain beamforming operation for a uniformly spaced, linear array. Note that in this form it applies equally well to broadband signals so long as there is no dispersion in the wave medium over the length of the array. If one takes the temporal Fourier transform of Eq. (2-17), one obtains

$$\bar{B}_m(f) = \sum_{n=0}^{N-1} a_n \bar{E}_n(f) e^{-j2\pi f\tau_{nm}} \, , \tag{2-18}$$

where $\bar{E}_n(f)$ is the Fourier transform of $e_n(t)$. This equation will be the basis for the frequency-domain techniques of Section II-C.

The next two sections contain descriptions of various implementations of the basic beamforming equation in the time and frequency domains. The chapter concludes with a discussion of the strengths and weaknesses of digital beamforming.

B. Time-Domain Beamforming

Delay-sum beamforming from a linear array of N sensors is defined by Eq. (2-17). A completely analog beamformer can provide the exact τ_{nm} defined by Eq. (2-6). However, if errors are not to be introduced in a discrete-time implementation, the outputs of the sensors must be sampled at a frequency $f_S = 1/T_S$ which is high enough to satisfy Eq. (2-6) for all desired look directions θ_m; many beamformers do not meet this requirement because of sampling rate limitations[7]. Those beams for which the sampling period allows Eq. (2-6) to be satisfied exactly are termed *synchronous* beams. For lowpass beamforming the sampling rate is usually set at four to six times the highest frequency of interest. This usually requires the forming of non-synchronous beams with their concomitant errors[8], although the effect of the errors is often quite small.

If the beams are formed at a frequency $f_0 = 1/T_0$, then Eq. (2-17) becomes

$$b_m(kT_0) = \sum a_n e_n(kT_0 - M_{nm}T_S) \ , \ k \in \text{integers}, \tag{2-19}$$

where M_{nm} is an integer which best approximates the desired delay time, i.e.,

$$\tau_{nm} - T_S/2 < M_{nm}T_S < \tau_{nm} + T_S/2 \ . \tag{2-20}$$

For proper reconstruction of a beam's waveform the beam formation rate f_0 must be at least as great as the Nyquist rate.

Some disadvantages of delay-sum beamforming are:

1) The sensors must be sampled at a rate several times higher than the Nyquist rate to provide reasonable approximations to the required delay times for beamforming.
2) Large amounts of memory are required to store the sampled data from large arrays when long time-delays are desired.
3) If the beamformer is located a great distance from the analog-to-digital (A/D) converters, high cable bandwidths are required for large arrays.

Note that the computations involved in the actual beamforming operation can be done at the beam formation rate f_0 even though the data are sampled and stored at the higher rate f_S.

In **partial-sum** or **sum-delay** beamforming, sensor data are added to the appropriate sums as they are sampled, i.e., the samples are not stored for later computation; rather, partial sums are stored until a complete beam is formed every T_0 seconds. This requires that a new partial sum for each beam

be initialized every T_0 seconds and has the effect of reducing memory requirements at the expense of increased control complexity. The number of partial sums P_m required to form the m-th beam at a rate f_0 is given by

$$P_m = f_0 \, MAX_n(\tau_{nm}) \tag{2-21}$$

where $MAX_n(\tau_{nm})$ is the maximum delay required to form the m-th beam. The total number of partial sums P_T required to form N_B beams is

$$P_T = \sum_{j=1}^{N_B} P_m \, . \tag{2-22}$$

For a conventional delay-sum beamformer the amount of memory required M_T is given by

$$M_T = N f_S \, MAX_m(\, MAX_n(\, \tau_{nm} \,)) \, , \tag{2-23}$$

although this can be reduced somewhat with a clever beamforming algorithm.

A problem with both delay-sum and sum-delay methods is the need to sample at a rate higher than the Nyquist rate. To avoid this drawback, one may generate the required samples by interpolation of data sampled at the lower Nyquist rate[9]. In fact, the interpolation can be performed either before or after the beamforming operation. This lowers the requirements for the A/D converter, memory, and cable bandwidth. If the sampled data are passed through a perfect lowpass filter, the interpolation is exact. The usual approach is to pass zero-padded samples through a Finite-duration Impulse Response (FIR) filter designed to act as a lowpass filter. The zero-padding operation consists of placing the proper number of zeroes between each pair of data samples; e.g., if the desired sampling rate is five times the Nyquist rate, four zeroes are inserted between every pair of samples. Whether the interpolation should be done before or after beamforming depends on the particular implementation. This issue is addressed more fully by Mucci[10].

Additional easing of the hardware requirements can be made in bandpass systems by complex-sampling and interpolation techniques[11]. Three common methods are analytic signal, second-order, and quadrature sampling[12]. Because the samples are complex, the phase information is retained even though the sampling rate might be much lower than the center frequency. A further complex sampling technique is the shifted sideband beamformer discussed by Pridham and Mucci[13].

A hard-clipping technique is sometimes used where detection is the main objective. This DIMUS technique[14] is easily implemented with digital circuitry since the signal is simply binary. When properly executed the technique usually suffers only a small S/N loss.

C. Frequency-Domain Beamforming

Since Eq. (2-5) is for single frequency signals, it may be written in a slightly different format, namely

$$b_m(t) = \sum_{n=0}^{N-1} [a_n \tilde{e}_n(t) \exp(-j2\pi\Phi_{nm})] + c.c. , \qquad (2\text{-}24)$$

where the complex sample $\tilde{e}_n(t)$ is given by

$$\tilde{e}_n(t) = E_0 e^{j[\omega(t + (X_n \cdot K)/c)]} ,$$

and

$$\Phi_{nm} = n\frac{fd}{c} \sin\theta_m = f\tau_{nm} .$$

Thus, we may view the beamforming operation as a sum of weighted and *phase-shifted* sensor values all sampled at time t. Phase-shift beamforming is designed for narrowband signals: the processing occurs in the frequency domain: as such, no actual time delays are required, and the steering precision is set by the attainable phase shifts, not by the sampling rate. This method is illustrated in Fig. 3. Note that the phase shift is a function of frequency and is usually set to the center frequency of the narrow band of interest. This method requires N complex multiplies for each beam to yield a rate of NN_Bf_0 complex multiplies per second.

One can view Discrete Fourier Transform (DFT) or Fast Fourier Transform (FFT) beamforming as phase-shift beamforming applied at several frequencies in a band of interest. If we approximate Eq. (2-18) by using a discrete Fourier transform, the resulting equation reads

$$\bar{B}_m(k) = \sum_{n=0}^{N-1} a_n \bar{E}_n(k) e^{-j2\pi k f_s \tau_{nm}/L} , \quad k = 0,1,\ldots K-1 , \qquad (2\text{-}25)$$

where the L-point DFT of $e_n(t)$ is given by

$$\bar{E}_n(k) = \sum_{l=0}^{L-1} e_n(lT_s) e^{-j2\pi kl/L} . \qquad (2\text{-}26)$$

This procedure is illustrated in Fig. 4.

The advantages of this procedure are that the data need be sampled only at the Nyquist rate and that the DFT can be done efficiently with an FFT algorithm[15] in some cases. A major disadvantage stems from approximating the Fourier transform by an integral over a finite time. Imagine a monochromatic waveform propagating across the array at an oblique angle: since the transform is over a finite period of time, the various transforms at the sensors

will operate on different portions of the received waveform due to the propagation delays. To avoid inaccuracies, the time window of the transform is usually ten times the maximum array propagation delay or longer. This greatly increases the storage and calculational requirements for the processor. Furthermore, the DFT of $b_m(t)$ is not equal to $\tilde{B}_m(f)$ except for large time windows (large L).

If the time delays τ_{mn} are such that Eq. (2-25) can be written as a DFT, then the computation may be done with the efficient FFT algorithm. All beams are produced at once by this method, although their directions are not steerable. This method is inefficient if only a few beams are desired or if there are fewer than approximately 100 sensors.

A recently developed frequency domain technique enables efficient interpolation of missing sensor values[16]. It utilizes a computationally efficient two-dimensional FFT algorithm and therefore requires uniform sensor spacing, but it produces as output beamformed time sequences which may be used in coherent signal processing, e.g., matched filtering. It may be thought of as equivalent to an interpolating delay-sum beamformer.

D. General Considerations and Digital Implementations

Any time-domain beamformer, be it analog or digital, must perform the same basic set of operations. The signals from the sensors are usually sampled and shaded (weighted), they are then routed to the proper locations via some network (hardware or software), the proper time delays or phase shifts are applied (again via hardware or software), and finally the signals are summed (at the proper location or time).

Any frequency-domain beamformer must also fulfill a basic set of operations. The sensor signals must first be transformed to the frequency domain: this is usually done via a Fast Fourier Transform over a suitable time interval. The beamforming is done by multiplying the data in each frequency bin by the proper (complex) phase and then summing. This is done for each frequency bin and each beam direction. The data for each beam may then be transformed to the time domain for further processing.

Any implementation of a beamformer must be made within a set of constraints imposed by the application and the available technology. Some application constraints are:

1) The desired array gain and response pattern. These are determined by the number of sensors and their configuration. The spatial arrangement of the sensor array is primarily determined by the application and the platform: linear, planar, circular, random and conformal arrays have all been employed. Linear arrays are commonly towed behind a ship which may also have active capability, and both linear and planar arrays are used in bottom mounted systems. Circular arrays are commonly hull-mounted and are usually part of an active system. Random arrays occur when sonobuoys are dropped from a plane or ship. (Note that all arrays are random to some degree, e.g., towed arrays are never exactly linear because of array motion. This departure from exactness must be accounted for in the beamforming operation.) A recent technique is to use conformal arrays, i.e., sensors which conform to the surface of the vessel and cover a large area in order to maximize the amount of received acoustic energy.
2) The number of beams and their directions. The upper limit on the number of beams is set by the ability of the post-processing system to handle the information load.
3) The center frequency and bandwidth.
4) Processing time available.
5) The environment.
6) The desired lifetime. This is of primary importance for sonobuoys and is limited by power consumption and the storage density of batteries.
7) The budget.

A list of the constraints imposed by the available technology might include:

1) The type, linearity, bandwidth, noise level, and dynamic range of the sensor signals. The dynamic range of the signal at the receiver in an active sonar system can exceed 90 dB[17]. Automatic gain control or time-varying gain done prior to beamforming can be used to handle this problem, although a digital signal processor with enough bits to handle the expected dynamic range is sometimes used. Other systems use a non-linear response function to reduce the processing load.

2) Signal transfer and cabling requirements. High bandwidths and long transmission distances are difficult to obtain. Digitized data can be sent without errors but at the cost of a high bandwidth requirement.
3) Data domain: analog, digital, optical, electrical, etc. This is often determined by the available device technology.
4) Amount of data storage available. This can be a severe constraint for systems with many sensors.
5) Maximum dynamic range available. Digital systems have little problem with this once the data have been digitized, but analog-to-digital converters are expensive and consume large amounts of power.
6) Maximum processing rate available given size, power, time, and weight constraints from application requirements. This is the driving force behind the miniaturization of digital circuitry.

After considering all the constraints, most system designers choose binary digital processing. This is primarily because of its flexibility, dynamic range, and the availability of standard building blocks. A more complete list includes the following benefits:

1) The techniques are well-established and understood.
2) The systems can be designed for flexibility (programmability). This allows for array conformation corrections, minor software corrections, and dynamic parameter specification.
3) The dynamic range can, in theory, be as large as desired.
4) Data storage is simple and data corruption is a problem easily solved.
5) Memory densities are large and growing larger.
6) The system is very stable, i.e., once the signals are digitized, one need not worry about the effects of temperature and other fluctuations on the processor.
7) Digital systems are becoming faster and smaller.

Some constraints are:

1) The actual dynamic range is limited by the availability of ADC's with the requisite combination of high speed and large dynamic range. Current systems often use automatic gain control or time-varying gain to reduce the requirements for the ADC's.

2) Large dynamic range and number of sensors requires a high bandwidth for the cable if the sensors and ADC's are situated a great distance from the processor.
3) The rapid and large gains made in digital technology are not likely to continue: any further advances will come at great effort and expense as feature size and thermal limits are approached.
4) New architectures, such as parallel processing, have been proposed to provide higher computation rates but these methods currently have high costs and the architectures are usually application-specific.
5) Electrical connections in more than two dimensions are extremely difficult to fabricate, thus limiting the circuit densities attainable.

Before digital computers attained such popularity, signal processing was done in the analog domain. It is ironic that the very technology that enabled digital techniques to supplant analog systems has, in recent times, set the stage for a resurgence in analog signal processing. Micro-circuit fabrication techniques can be used to make small, stable, and efficient analog systems such as surface-acoustic-wave (SAW) devices and charge-transfer-devices (CTD's). These can be used to advantage in analog optical or electronic signal processing systems[18]. The fabrication techniques have also made possible linear and planar arrays of micron-sized photodiode detectors and linear arrays of light-emitting-diode (LED) or laser diode sources. What optical processing still needs is a fast, dense, efficient, two-dimensional spatial light modulator. Systems using current spatial light modulator technology are discussed in the next chapter.

III. OPTICAL BEAMFORMING

A. Introduction

Present-day sonar systems operate under severe constraints. Space on board a sea-going vessel is almost always in short supply, and beamforming systems occupy a significant portion of available volume. Since the received signals are becoming weaker and weaker, more and more sensors must be used to obtain suitable signal-to-noise ratios: this implies a larger and more complex beamformer. One can envision systems with a hundred- or even thousand-fold increase in the number of sensors. The signal processors attached to this system must not occupy a commensurately larger volume and therefore must

have orders of magnitude greater processing capability. The constraints are even more severe for expendable systems: although the number of sensors is usually small, they must be serviced by an extremely efficient processor since the power is supplied by batteries; in addition, the package is usually very small, with most of the volume filled by the power source. Not only must sonar systems satisfy the constraints imposed by the processing load and satisfy the application requirements, they must also be economical and reliable.

Optical signal processing has several qualities which recommend it for processing multiple streams of data in real time:

1. Signals propagate with the speed of light.
2. Connections and data flow for two-dimensional information are inherently parallel.
3. Complicated three-dimensional connection schemes are possible.
4. Analog multiplication at rates of 10^{15} multiplies per second is possible.
5. Powerful processors can be built inexpensively, i.e., small, lightweight, fast processors which consume little power. This fact is becoming increasingly important because of the expected processing loads of envisioned systems.
6. Optical beamforming might provide a natural interface to fiber optic sensors.

Since it is our intent to evaluate the extent to which these advantages can be applied to *real* sonar systems, we must identify any potential disadvantages. Some obvious shortcomings of analog optics are that:

1. Linearity is a function of the physical properties of particular devices and achieving it over a wide dynamic range is often difficult.
2. Time delays longer than a few tens of nanoseconds are difficult to obtain.
3. It is difficult to control phase shifts precisely.
4. Using the tremendous multiplication rates often requires time-scale compression, and this implies some sort of high-speed read/write memory system and its concomitant problems.
5. Interfacing an analog optical processor with a system that was designed for digital signal processing can be difficult. This problem

becomes acute when the data must be transformed from the analog to the digital domain and back many times.

6. Poorly designed systems are subject to stability and reproducibility problems.
7. Improperly designed analog systems tend to be less flexible than programmable digital systems.

The choice of which algorithm to employ for an optical beamformer depends on whether the operation is done in the time or frequency domain and on the center frequency of interest. It is difficult to apply time delays much longer than a few tens or hundreds of nanoseconds directly in the optical domain. Thus, in a time-domain implementation at low frequencies (sonar), the use of optics should be limited to signal routing and perhaps shading, whereas at high frequencies (radar) it might be possible to implement the delay operation with fibers.

An increased potential for optical processing exists for frequency domain beamforming due primarily to the multiplication capability of optics. One possible implementation is a discrete Fourier transform beamformer in which the data-stream into the processor is in the frequency domain and the phase shifts are applied by the DFT operation in an optical vector-matrix multiplier, i.e., the frequency domain data form a vector and the necessary phase shifts are stored in the matrix.

Until recently, there has been little effort to build practical optical beamforming systems, although some preliminary concept and development work has been done[19]. A Photo-Acoustic Space Time (PHAST) beamformer feasibility model was developed by General Electric Company and delivered to NAVAIRDEVCEN in 1979[20]. It provided continuous beam steering in a time-domain, phase-shift mode. The PHAST beamformer was designed to be used in a sonobuoy but it consumed too much power, due primarily to its use of an acousto-optic Bragg cell.

The remainder of this chapter is devoted to a discussion of several opto-electronic approaches designed and implemented at NRL that point to some promising directions for research and development.

B. Time-domain Optical Beamforming

We describe three methods for implementing a time-domain beamformer using optical techniques. The first is a space-integrating method, and the last two are time-integrating methods.

Space-Integrating Method

The schematic diagram of this beamformer is shown in Fig. 5. The major components are a light source (usually a semiconductor laser diode, e.g., Hitachi HLP-1400), collimating optics for producing a uniform two-dimensional optical beam, a multi-transducer light modulator, which in the figure is an acousto-optic (AO) Bragg cell with one transducer per sensor, an imaging system, a computer-generated hologram (CGH) (to be described later), a spherical lens used in a Fourier transform configuration, and a parallel readout detector array for producing the beam samples.

In the arrangement of Fig. 5 the laser diode must be pulsed at the sampling rate of the incoming data stream, but due to the traveling wave nature of the data stream in the AO cell, the pulsewidth must be less than the sampling period to avoid overlap of the information in one data sample with that of an adjacent sample. The time window of the AO cell must be long enough to accommodate the longest required delay between any two elements of the hydrophone array. Also, the bandwidth of the AO cell must be high enough to resolve individual data samples. These last two requirements imply a minimum time-bandwidth product for the acousto-optic cell.

In the AO cell the spatial position along the acoustic propagation direction encodes the time delay via the formula $t = x/v$ where v is the acoustic velocity in the cell. The time delays τ_{nm} can now be translated into positions in the x-y plane containing the multi-transducer AO device as follows:

$$\tau_{nm} \rightarrow (x_{mn}, n\Delta y)$$

where Δy is the transducer inter-channel spacing and x_{mn} is the sample location that is determined by both the hydrophone element n and the beam m. The task of the beamformer is to sum the light intensities transmitted by the multi-transducer AO cell at locations $(x_{mn}, n\Delta y)$ for all n to produce the m-th beam.

The computer-generated hologram lies in the image plane of the AO cell and consists of apertures with gratings of different frequencies inside them. For the m-th beam, the CGH mask will have apertures at locations $(x_{mn}, n\Delta y)$ for all n, each containing a grating of unique frequency $(f_x^{(m)}, f_y^{(m)})$. The Fourier transforming lens sums the light intensities transmitted by all apertures and directs them to a location (x'_m, y'_m) in the output (Fourier transform) plane of the processor that is determined by the frequency $(f_x^{(m)}, f_y^{(m)})$. A detector at that location will produce the desired beam output $b_m(t)$.

A selection of a different beam, e.g., $b_k(t)$, will involve a new set of sample coordinates (x_{kn}, $n\Delta y$) and a new grating frequency ($f_x^{(k)}$, $f_y^{(k)}$) for the CGH mask apertures. The beam is now produced by a detector placed at (x_k', y_k'). Thus all the desired beams can be calculated simultaneously. It should be noted that the location of an individual beam is determined completely by the corresponding grating frequency and hence can be chosen to conform to available detector geometries or to minimize inter-beam crosstalk. New samples of all the beams are calculated simultaneously every time a new sample of the array data is introduced.

The multi-transducer AO cell can be replaced by a corresponding array of delay lines that address an optical medium. An example is a device developed by Xerox known as the integrated total internal reflection (TIR) spatial light modulator[21], which consists of a silicon VLSI delay line that induces index-of-refraction changes in an electro-optic material, such as lithium niobate, to modulate an optical beam in a manner analogous to an acoustic-optic device. The advantage of this approach is that the data are not in the form of a continuously traveling wave, so the laser diode light source can remain on as long as the delay line voltages are held steady. The light is turned off only when the data are shifted in the delay line (e.g., to introduce a new data sample).

Time-Integrating Methods

In the previous architecture, the multi-transducer AO cell was used as a delay line storage element with the CGH mask providing the tapping. In the time-integrating class of architectures, no storage is necessary for the input array data. Each sample of the array data is used in the partial sum of the beam calculation as dictated by the algorithm. The first time-integrating architecture we describe operates in a blocked mode, where a beam is produced only after all the samples required in the summation are accumulated. The second architecture operates in a continuous mode, where one sample of the output beam is produced every time a new sample of the array data is introduced into the processor.

Optical Cross-Bar Architecture

The schematic diagram of this optical architecture is shown in Fig. 6 and is an implementation of the delay-sum beamformer discussed in Sec. IIB. The arrangement consists of an array of light sources such as a linear array of LED's as shown in the figure (one for each hydrophone in the array), an astigmatic lens that spreads light in the horizontal direction and images it in the

vertical direction, a two-dimensional dynamic matrix mask (e.g., Radio Shack LCTV, or Litton Industries LIGHT MOD^{TM}), another astigmatic lens that images in the vertical direction and focuses light in the horizontal direction, and a linear time-integrating detector array to produce the beam samples. The matrix mask contains one row for each hydrophone (i.e., one row for each LED) and one column for each beam (i.e., one column for each detector element). Thus for an N-element hydrophone array forming M beams the matrix mask will contain $M \times N$ elements. The hydrophone outputs are applied in parallel to the linear LED array one sample at a time. The matrix elements effectively decide which time samples of the hydrophones contribute to a given beam. The operation of this architecture can be explained with an example of a four-element array.

The beam along $\theta = 0$ is formed when all of the hydrophone outputs are added together without any delays. To form the beam along $\theta = \theta_1$, adjacent hydrophone outputs are added with a delay equal to the sampling interval for the array; thus, the samples of hydrophones 1, 2, 3, and 4 are delayed by 0, T_s, $2T_s$, and $3T_s$ and added to form the first beam. The beam for $\theta = \theta_2$ is formed by introducing delays in multiples of twice the sampling interval; thus, the samples are delayed by 0, $2T_s$, $4T_s$, and $6T_s$ and then added. This is done by switching the transmittances of the mask elements at the appropriate times. The proper times for switching a 4×4 matrix device to form four beams with a four-element array are shown in Fig. 6, where $t_2 - t_1 = T_s$, $t_3 - t_1 = 2T_s$, etc. One sees that after four cycles, the detector element that integrates the light transmitted by the second row produces the beam along $\theta = \theta_1$. This architecture operates in a block mode, i.e., the beam samples are calculated only after the required samples from all the elements have been acquired.

Alternatives to the linear array of LED's include: i) Electro-optic spatial light modulators such as electroded PLZT plates or the TIR device mentioned in the previous section. The data can either be transmitted in parallel to the PLZT electrodes, as shown in Fig. 6, or as a multiplexed serial data stream into the delay line of the TIR device. ii) An array of acousto-optic point modulators. iii) A single AO deflector that accepts a multiplexed serial data stream. Due to the travelling wave nature of the data, the light source must be pulsed to freeze the data pattern at the appropriate times.

An implementation of this architecture is discussed in the next chapter.

Optical Accumulate-and-Shift Architecture

In this version of the sum-delay architecture the main component is a CCD detector array operated in an accumulate-and-shift mode. The principle can be illustrated with an example of a linear detector array configured to form a beam in the $\theta = \theta_1$ direction for a four-element hydrophone array. The shift rate of the CCD array is synchronized with the sampling rate of the hydrophone array, i.e., the CCD shifts the charges by one pixel every sampling period and then adds the charge generated by the new sample to the partial sum represented by the existing charge at that site. The length of the CCD shift register must be equal to the total number of time samples required to form that beam.

Figure 7 is a schematic diagram of the processor. It contains a linear light modulator array (e.g., LED's, PLZT, or TIR devices), a CGH optical element, and an accumulate-and-shift CCD detector array with the shift registers along the direction of the LED array. The CGH is designed to deflect light from each LED to the appropriate detector pixel, which is determined by the look direction for the beam. The figure shows a four element array to form four beams in the directions discussed in the previous example.

One can see that, after an initial delay needed to fill the CCD shift registers, this system calculates a new sample of the output beam every time a new sample of the input is applied. Thus this architecture operates in a continuous mode as opposed to the block mode of operation for the time-integrating architecture described previously.

We have designed and are building an implementation of this architecture. It is an eight-channel sum-delay beamformer using optical fibers and fiber splitters for signal routing to a charge-transfer-device. In addition to utilizing the routing capabilities of optics, this implementation has potential advantages of high EMI immunity, smaller volume, lower power (< 10 mW), environmental robustness, and simpler electronics. It also has potential for much higher frequency applications (e.g., radar) if a fast charge transfer device (e.g., GaAs) is used.

C. Frequency-Domain Optical Beamforming

Optical beamforming in the frequency-domain is possible in at least one form because the operation can be cast in the form of vector-matrix multiplication. The frequency-transformed data of one sensor form the (complex) vector, and phase shifts equivalent to beamsteering delays in the proper directions form the (complex) matrix. The results are stored and the next vector

is processed until all the sensor data have been used and all the beam channels formed.

The basic operation performed by the vector-matrix processor is a complex multiplication. The product of two complex numbers, z_1 and z_2 may be written as

$$z_1 \cdot z_2 = \left(z_1^r z_2^r - z_1^i z_2^i\right) + i\left(z_1^r z_2^i + z_1^i z_2^r\right) , \qquad (3\text{-}1)$$

where the superscripts stand for the real and imaginary parts. In the optical domain this operation can be done in two ways: a coherent system would use some sort of interference technique to obtain the difference term; an incoherent system must use intensity values with some sort of coding scheme to perform negative number arithmetic. While the first method is more intuitive and perhaps aesthetically more appealing, it has the limitation that the entire dynamic range must be encoded in one wavelength, i.e., 2π radian. For more than one or two bits of precision this translates into severe mechanical constraints on the encoding process. This is commonly done with holograms, but currently available techniques are still rather limited.

The second method may be implemented in a straightforward way using four real multiplications. In this scheme, negative numbers are represented as positive values below some bias level which represents zero. A complex phase is encoded as an array of four transmittances, and vectors are encoded horizontally. Complex multiplication consists of transmitting intensity levels corresponding to the real and imaginary parts of a vector through the following pattern

$$\begin{pmatrix} R & -I \\ I & R \end{pmatrix}$$

so that the real part is cast across the left column of the array (R and I) and the imaginary part across the right column (-I and R), and then summing the horizontal terms to yield a vector encoded vertically with the real part uppermost. This type of architecture is shown schematically in Fig. 8. An experimental implementation of this approach is discussed in the next chapter.

D. Interfacing

Most optical signal processors are analog, whereas much electronic signal processing is done digitally. Conversions from one data domain to another are usually expensive in time and power. Melding the two approaches into a successful hybrid system requires careful design and engineering: a properly

designed system will keep the number of conversions to a minimum. Under such constraints the proper location of the interface between the optical and digital processors assumes critical importance and must be considered at the start.

Some other considerations which should be made at the beginning of system design are:

1. Analog optical systems are generally limited in dynamic range, eight bits being a common figure. For data with a higher dynamic range, some form of compression or gain control must be used.
2. Processing in the analog domain is generally much faster than in the digital domain. This implies some sort of multiplexing from parallel digital input/output lines to a serial analog line so that the digital system can fully utilize the optical processor's potential. This also implies a time-scale compression.
3. A particular problem might be solved more efficiently with the replacement of digital electronics by analog electronics at critical points. This has the effect of reducing the number of data conversions and tailoring the system to the optical processor for greater efficiency.

The importance of these considerations will become apparent in the discussion of the implementations in the next chapter.

IV. OPTICAL BEAMFORMING: IMPLEMENTATION DETAILS AND EXPERIMENTAL RESULTS

This chapter describes several implementations of optical beamformers which were developed at NRL. The first is a time-domain delay-sum beamformer[22], the second uses the accumulate-and-shift architecture, and the third is a frequency-domain vector-matrix beamformer.

A. Implementation of an Optical Cross-Bar Beamformer

We have implemented a time-domain delay-sum beamformer (described in Sec. IIIB) using a low-cost, low-power, liquid-crystal television (LCTV)[23] in an optical cross-bar switch configuration. Power consumption in the LCTV is about 10 μW/pixel, and for 122 $\times$ 148 pixels the total consumption is 180 mW.

This beamformer was successful in producing beams in the proper manner, but there are several limitations of the implementation which we identified.

We first discuss the algorithm employed to implement the delay-and-sum operation. The array contains eight sensors, and the beamformer produces eight beams in parallel. In Fig. 9, the beamforming operation is depicted as a set of delay lines with taps to form the beams. The beams shown correspond to broadside (0), endfire (4), and six beams (±1, ±2, ±3) spaced 0.25 apart in $\sin\theta$-space; e.g., the look direction for beam ±1 is ±14.5 degrees. The time axis in Fig. 9 is shown as being continuous, but for the demonstration the data were sampled at a rate of $5f_0$. Sampling at rates higher than the Nyquist rate reduces beam-steering errors due to quantization[24], i.e., one must select those samples which lie nearest to the tap points in Fig. 9; a higher sampling rate reduces the error. The endfire beam determines the longest delay and thus determines the maximum length of delay line required (or equivalently, the amount of memory). This delay is (N-1)d/c seconds which corresponds to $(N-1)d/(cT_S) + 1$ samples, where $T_S = 1/(5f_0)$. Since $d/c = 1/(2f_0)$, the number of samples required to form one output sample of the endfire beam is (N-1)(5/2) + 1, or 19 for N = 8. A list of the sensor samples required to form the eight beams is given in Table 1.

The beamforming algorithm is as follows: (a) The sampled sensor values are stored in a buffer. (b) They are then presented as an eight-element optical vector to a matrix mask which blocks or passes the sensor samples according to the table. (A few of these masks are shown in Fig. 10.) (c) The

Table 1. Sensor Values Required at the Listed Sample Times to Form Eight Beams

	SENSOR							
BEAM	0	1	2	3	4	5	6	7
0	0	0	0	0	0	0	0	0
1	0	1	1	2	2	3	3	4
2	0	1	2	3	5	6	7	8
3	0	2	4	5	7	9	10	12
4	0	3	5	8	10	13	15	18
-1	4	3	3	2	2	1	1	0
-2	8	7	6	5	3	2	1	0
-3	12	10	9	7	5	4	2	0

t / $5f_0$

transmitted values are added in running sums in a detector array. (d) Steps (b) and (c) are repeated until the last beam (endfire) is formed. (e) The running sums are then presented as an eight-element vector of beam output

samples. This operation is repeated to form a temporal sequence of beam output samples occupying a total interval $1/f_0$.

A schematic diagram of the experimental arrangement is shown in Fig. 11. The general arrangement is that of a vector-matrix multiplier: a sheet beam of laser light is modulated by a total internal reflection (TIR) electro-optic device[21] with multiple inputs to produce a vector representing the various sensor values; the matrix mask is generated by a two-dimensional spatial light modulator (2-D SLM), i.e., the LCTV; cylinder lens CL2 spreads the input vector vertically over the LCTV and CL3 sums across sensors and transmits these values onto the detector array where the running sums are performed. Synthetic data representing the sampled and hard-clipped (binary) response of eight sensors to sinusoidal plane-waves approaching from an angle θ are presented to the TIR modulator by the microcomputer which also provides the synchronization signals for the experiment. (Hard-clipped signals are used in large systems because of the simplicity of the hardware; normally, this is done only for arrays of about 30 or more sensors to minimize the distortion in the response pattern[25]. We chose hard-clipping for ease of implementation and for demonstration purposes.) The matrix pattern or routing mask for the 2-D SLM is generated by the video output of the microcomputer's graphics system. A minicomputer controls the detector array. To improve the S/N, the vector-matrix products are first formed on the detector and integrated, the mask is then blanked and the background signal integrated, and finally the two integrated frames are subtracted to obtain the desired signal.

The array response pattern (average output power as a function of incidence angle θ) for a broadside beam ($\theta_m = 0$) is shown in Fig. 12. The dashed curve corresponds to the theoretical pattern for an unclipped signal, the solid curve to the theoretical pattern for a clipped signal, and the filled squares show the experimental results. The distortion in the theoretical pattern for the clipped case relative to the linear case is apparent in Fig. 12; nonetheless, the results demonstrate the capability of the optical approach to produce the theoretically expected pattern. The S/N is about 8 and is limited by the noise in the LCTV.

The primary faults with this particular liquid-crystal device are its observed slow response time (~100 ms/frame), the instability in the amplitude of its response due to temperature fluctuations and RF jitter (~3 s integration time needed to smooth it), and the rastering of the pixel control voltages. These proved to be serious limitations: excessively long integration times were required to obtain reasonable response.

A better liquid crystal device would improve the response time and signal-to-noise ratio, but a major inefficiency exists in the algorithm we chose, as many data samples are used several times in the course of generating one period of five output samples. Because of the limitations of this approach we are no longer pursuing it. Our intent was to develop a low-cost, low-power, compact beamformer; we have recently identified an architecture which seems much more promising and we discuss it in the next section.

B. Implementation of a Partial-Sum Beamformer

A beamformer that we are presently breadboarding is designed around fiberoptic couplers. The partial-sum algorithm on which it is based was discussed in Sec. III-B for the case of a hologram instead of optical fibers. This beamformer has low power requirements, uses optical isolation of the sensor channels, and forms multiple beams.

The major components used to implement this beamformer are LED's, fiberoptic couplers, and a photodetector/CCD multiplexer (MUX). Figure 13 is a schematic of a design that generates eight beams from an eight sensor linear array in which the beams are read out serially. If the sensors do not generate optical intensity signals, then LED's are used to convert the electical signals to the optical domain. The optical signals are routed to the appropriate detectors via fiberoptic couplers: for eight beams each signal is split eight ways. Some of the detectors receive signals from several sensors; this can be done simply by butting the several fiber ends to a single detector. The CCD MUX samples the outputs of the photodetectors at an appropriate clock rate; the charge packet in each cell of the CCD represents a beam partial sum. The beams are read out as a time sequence at the CCD shift rate.

The operation of a more general system consisting of a linear array of N sensors and a beamformer generating M beams is as follows. The CCD is operated in an accumulate-and-shift mode: the charge accumulated in an element during the sample time is shifted M elements whereupon new charge from the next detector (if present) is added to the packet. The CCD is divided into blocks of M elements; each element in a block corresponds to a beam partial sum. The beam which requires the longest delays determines the number of blocks required and is a function of the sampling rate, the number of sensors and their spacing, and the beam look directions: for a linear array with sensor spacing $\lambda/2$, a sampling rate n times Nyquist, and an endfire beam, the formula is $N_{blocks} = n(N-1) + 1$. The total number of elements required for the CCD is then MN_{blocks}. The detector outputs are positioned along the CCD

so that the desired beams are formed. When a block of charge packets reaches the end of the CCD, each charge packet (now a complete beam sample) in the block is read out during the next shifting operation.

Our breadboard version of this beamformer uses off-the-shelf components to generate three beams from eight sensors. A more complete set of beams is not formed because of the size of the CCD MUX (manufactured by EG&G Reticon) which is 32 elements long. A 26-element photodetector from Silicon Detector Corporation was mounted on the same chip carrier as the CCD. The two are wired together by flying leads to form the photodetector/CCD MUX as shown in Fig. 14. Twenty-four fiber ends from eight ITT 3×3 star couplers are connected to the photodetectors. The input ends of the fibers are connected to Fujitsu LED's. While this beamformer generates only a partial set of beams, it will demonstrate the performance levels attainable with a fiberoptic beamformer.

The CCD and the LED's consume most of the power in this beamformer. The power consumption in the CCD is split between the drivers and the output buffer. The buffer consumes about 5 mW, while the power consumption of the drivers depends on the capacitance of the CCD elements. For an eight-element beamformer forming eight beams, the number of elements required is 232. For an element capacitance of 2 pF, 10 V operating voltage, and a shift rate of 64 kHz, the driver power is 3 mW ($C \times V^2 \times f$). Therefore the total CCD power consumption is less than 10 mW. The LED power requirement is found by dividing the power required to saturate 8 CCD elements by the total LED-fiberoptic efficiency. This efficiency depends on three elements: the LED drivers, the LED's, and the star couplers. The LED drivers are current drivers and should have about 10% efficiency. The optical power which reaches the input to the star coupler should be about 1% of the power applied to the LED. The total power leaving the star coupler should be about 28% of that at its entrance port. These imply a requirement of about 10 mW for the LED's. Thus, total power consumption is expected to be approximately 20 mW; the breadboard version will give a more accurate measure of this figure.

C. Implementation of a Vector-Matrix Frequency-Domain Beamformer

Westinghouse (Baltimore) has built for NRL an acousto-optic vector-matrix multiplier to meet the following specifications:

1. Accepts a 128-element, complex-valued input vector with an amplitude dynamic range of three decades.

2. Multiplies the vector by a 128 × 128-element complex-valued matrix on a fixed mask.
3. Operates with a cycle time of 10 μs.
4. Produces complex-valued output vectors with 8-bit amplitude and phase dynamic range.
5. Fits in a nineteen-inch rack with a height of nine inches.

When operated as a frequency-domain beamformer, this vector-matrix multiplier is capable of producing 128 beam samples every 10 μs, but it can also be used in a mode where fewer beams are produced, e.g., 64, 32, etc. The beam-steering directions are fixed by the matrix mask and can be changed by replacing the mask.

The vector-matrix multiplier uses the following algorithm:

1. A vector is loaded into a photo-acoustic cell; the loading time is given by the ratio of the length of the cell to the acoustic wave velocity.
2. A light source is pulsed on for a duration long enough to give good detection statistics. This light is modulated by the vector in the photo-acoustic cell; the modulated light is again modulated by a matrix mask to form the vector-matrix products. The vector and matrix data are encoded according to the scheme outlined in Sec. III-C.
3. The products are detected and read out. The time required for this operation is set by the readout speed of the detector.

A schematic diagram of the vector-matrix multiplier is shown in Fig. 8. The pulsed laser diode and collimating optics provide a beam of light which is the medium for transporting the beamforming data to the CCD detector array. The light beam is focused to a line in the acousto-optic cell where it is modulated by the frequency-transformed sensor data. After expansion and recollimation, the modulated light beam is transmitted through the matrix mask which contains the beam phase-shift information. The products are summed by a lens system, and then imaged onto the detector.

The system was designed to accept digital data as input and to produce digital data as output, but it operates in the analog domain, so provision must be made for the necessary data conversions. The input pre-processing consists of a correction for the acousto-optic cell non-linearity, digital-to-analog conversion, exponential acoustic loss compensation, and RF modulation.

Post-detection processing consists of laser energy correction, vector bias correction, and matrix and fixed bias correction. As with any analog system which must mesh with a digital system, the data conversion processes are responsible for a major portion of the implementation complexity.

Table 2 compares a hypothetical digital frequency-domain beamforming system using VHSIC technology with the optical vector-matrix multiplier. While the optical system has lower precision, it consumes much less power and requires no cooling system.

Table 2. Frequency Domain Beamforming: 128 Beams in 10 Microseconds

	Optical Complex Vector Matrix	VHSIC: IBM CMAC
Power	≈10 W	≈250 W (64 CMAC Chips)*
Volume	≈2 Cu. Ft.	≈2 Cu. Ft.
Precision	8 bits	12 bits

*Complex Multiply and Accumulate chips arranged in phase-shift beamforming architecture. Required additional control and functional circuitry not included in estimate.

It is possible to operate several vector-matrix beamformers in parallel if it is necessary to produce more beams or beams at a faster rate. Some disadvantages are the need for fixed masks, the requirement for a powerful, pulsed light source, and the high power consumption of RF power supplies. Nevertheless, should high-density, programmable masks become available, the vector-matrix architecture would become a powerful method for beamforming. We have recently taken delivery of this initial vector-matrix multiplier for test and evaluation.

V. SUMMARY AND CONCLUSIONS

Proposed requirements for future beamforming systems will tax the abilities of current technology. Current large-scale beamformers are generally digital with analog preprocessing of the sensor outputs. The need for greater gain implies an increased number of sensors in sonar systems and, hence, an increased processing load for virtually all components of the system; digital

systems will have a difficult time handling the processing load of systems with a hundred- or thousand-fold increase in the number of hydrophones. In addition, there are applications (e.g., sonobuoys) where a low-cost, low-power, compact beamformer would be extremely useful. Current digital technology cannot meet all projected needs, even for modest arrays.

We have described the mathematical foundations of the beamforming operation along with the theoretical processing requirements for various algorithms. This was followed by some general considerations for designers of beamforming systems and a presentation of the strengths and weaknesses of digital beamforming. The rationale for studying analog opto-electronic beamformers was presented along with several proposed architectures for time- and frequency-domain beamformers. After stressing the importance of the interface or system requirements, we presented several implementations of optical beamformers that have been or are being studied at NRL.

Beamformers are usually classified as time-domain or frequency-domain, according to whether the sensor data are delayed and then coherently summed or transformed to the frequency domain and then phase-shifted. Within each of these classifications are algorithmic variations that arise when one implements a general algorithm in specific hardware. The choice of algorithm is determined by the constraints imposed by the application and the available hardware. The most important of these constraints are the desired operating characteristics and the size and power limitations imposed by the available technology. Most system designers presently choose binary digital technology because of its flexibility, dynamic range, and the availability of standard building blocks. The primary limitations of digital techniques arise from the size and power requirements. For some applications processing speed is also a limitation.

Some of the advantages which optical technology brings to signal processing are: i) Connections and data flow are inherently parallel. ii) Connections can be made without mutual interference. iii) Three-dimensional connection schemes are possible. iv) Signals propagate at the speed of light. v) Analog multiplication at rates of 10^{15} multiplies per second is possible. vi) Powerful processors can be built which are small and consume little power. For any specific beamforming system one must minimize the effects of its disadvantages; some of the most important for analog optical technology are that: i) Linearity is a function of the physical properties of particular devices and achieving it over a wide dynamic range is often difficult. ii) Relatively long time delays are difficult to obtain. iii) It is difficult to

control optical phase shifts precisely. iv) Using the full multiplication rate usually implies the need for time-scale compression and its concomitant problems. v) Interfacing an analog system with a digital system can be difficult and unwieldy. vi) Poorly designed systems may have stability and reproducibility problems. vii) A poorly designed system can be inflexible.

Two developments improve the outlook for optical techniques: the increased use of optical fibers in sensors and communications, and the application of VLSI techniques to analog circuitry. The first development actually signals a need for processing techniques suited to the technology; the second provides a means of avoiding costly digital operations and of melding electronics with optics.

Three versions of a time-domain beamformer and a vector-matrix implementation of a frequency-domain beamformer were described in Chap. III. The degree of success of a particular implementation depends on the characteristics of the available device technology; thus, in Chap. IV, we described details of three implementations: a low-cost, low-power delay-sum beamformer, a sum-delay architecture using optical fibers, and a vector-matrix multiplier using acousto-optic Bragg cell technology.

The first implementation was built using a small liquid-crystal television set and a total internal reflection electro-optic modulator. While it generated beams correctly, it has limitations which make it unsuitable for a practical system. The more feasible approach being pursued for low-power beamforming uses optical fibers for signal routing and a CCD detector array in an accumulate-and-shift mode. The final technique uses a pulsed diode laser as a light source in a vector-matrix multiplier. The vector consists of frequency-transformed sensor data, and the matrix applies the appropriate beamsteering phase shifts. This approach is quite promising in that multiple modules can be operated in parallel. This processor is presently under test and evaluation.

As shown by the data in Table 2 and the details in Sec. IV-B, an analog opto-electronic beamforming system can provide significant reductions in power requirements for large-scale beamforming systems at a cost in volume comparable to or less than that of VHSIC technology. The early results of the fiber-optic/CCD beamformer indicate that this type of approach has potential advantages in low-power, low-volume applications over conventional digital technology. The current trend toward integration of optics with micro-electronics will surely benefit this approach. Optical systems should be considered for applications which require low power and volume and high speed but not high precision (greater than approximately eight bits). Note that low

precision does not necessarily imply low accuracy, which depends more on the algorithm.

The results of this research and those obtained by other workers indicate the potential advantages of opto-electronic processing techniques for certain beamforming applications and the importance of addressing the system integration questions from the start of the design process. This latter issue should also be addressed by the developers of new technologies. Little research has been done in this area; clearly it requires serious effort if future systems are to have the benefit of the best available technology.

In the near term this can best be done by identifying appropriate existing systems as test cases for insertion of an opto-electronic beamforming system. In the mid-term, advanced sonar system concepts need, at the initial stages, to include new technological approaches to signal processing. For the long term, optics needs to be integrated with other technological advances in signal processing, both analog and digital, to provide significantly enhanced performance levels in future sonar systems.

Recommendations for future work can be summarized along two lines. i) Technology development must be integrated into system design at the earliest possible stages. ii) Work on technology improvements should continue but be driven by specific application needs, e.g., speed in one case and power consumption in another.

REFERENCES

1. J. Cole, R. Johnson and P. Bhuta, "Fiber-optic detection of sound," J. Acoust. Soc. Am. 62, 1136-1138 (1977); J. Bucaro, H. Dardy and E. Carome, "Fiber-optic hydrophone," J. Acoust. Soc. Am. 62, 1302-1304 (1977).

2. G. Hetland, C.M. Davis and R.E. Einzig, "Optical sonar system concepts," October EASCON '79 Record, pp. 602-609.

3. W.C. Knight, R.G. Pridham and S.M. Kay, "Digital signal processing for sonar," Eq. IIB-52, Proc. IEEE 69, 1451-1506.

4. W.S. Hodgkiss and V.C. Anderson, "Hardware dynamic beamforming," J. Acoust. Soc. Am. 69, 1075-1083 (1981).

5. F.J. Harris, "On the use of windows for harmonic analysis with the discrete Fourier transform," Proc. IEEE 66, 51 (1978).

6. D. Casasent, "Optical processing for adaptive phased-array radar," IEE Proc. 127, 278-284 (1980).

7. G.L. DeMuth, "Frequency domain beamforming techniques," IEEE ICASSP 1977 Conference Record, pp 713-715.

8. Ref. 3, Eq. IIB-62.

9. R.G. Pridham and R.A. Mucci, "A novel approach to digital beamforming," J. Acoust. Soc. Am. 63, 425-434 (1978).

10. R.A. Mucci, "Digital beamformer implementation considerations," Electronics and Aerospace Systems Convention Conference Record (EASCON), 104 (1981). Our Sections II-B and C follow closely the discussion presented in this reference.

11. O.D. Grace and S.P. Pitt, "Sampling and interpolation of bandlimited signals by quadrature methods," J. Acoust. Soc. Am. 48, 1311-1318 (1970).

12. D.A. Linden, "A discussion of sampling theorems," Proc. IRE 47, 1219-1226 (1959).

13. R.G. Pridham and R.A. Mucci, "Shifted sideband beamformer," IEEE Trans. Acoust., Speech, Signal Processing ASSP-27, 713-722 (1979).

14. P. Rudnick, "Small signal detection in the DIMUS array," J. Acoust. Soc. Am. 32, 871-877 (1960); V.C. Anderson, "Digital array phasing," J. Acoust. Soc. Am. 32, 867-870 (1960).

15. E. Oran Brigham, *The Fast Fourier Transform* (Prentice Hall, Englewood Cliffs, N.J., 1974).

16. M.E. Weber and R. Heisler, "A frequency-domain beamforming algorithm for wideband, coherent signal processing," J. Acoust. Soc. Am. 76, 1132 (1984).

17. S. Patrick Pitt, W. Thomas Adams, and J. Kenneth Vaughan, "Design and implementation of a digital phase shift beamformer," J. Acoust. Soc. Am. 64, 808-814 (1978).

18. J.F. Dix et al., "Applications of c.c.d.s to sonar systems," IEE Proc. 127, 125-131 (1980).

19. G. Hetland, C.M. Davis and R.E. Einzig, "Optical sonar system concepts," October EASCON '79 Record, pp. 602-609.

20. M.T. Junod and A.M. Bates, PHAST (Photo-Acoustic Space Time) Beamformer Feasibility, Nov. 1979, Report No. NADC-80042-30, Naval Air Development Center, Warminster, PA 18974.

21. W.D. Turner and R.A. Sprague, SPIE Proc. 299, 76 (1981); R.A. Sprague, W.D. Turner, D.L. Hecht, and R.V. Johnson, SPIE Vol. 396, Advances in Laser Scanning and Recording, 44 (1983).

22. P.B. Rolsma, R.D. Griffin, and J.N. Lee, "Optical implementation of a time-domain beamformer," Opt. Lett. 11, 821-823 (1986).

23. F. Blechman, Radio Electron. 57(7), 39 (1986); H. Aldersey-Williams, Electro-optics 15(5), 55 (1983).

24. R.G. Pridham and R.A. Mucci, Proc. IEEE 67, 904 (1979).

25. V.C. Anderson, J. Acoust. Soc. Am. 32, 867 (1960); P. Rudnick, J. Acoust. Soc. Am. 32, 871 (1960).

APPENDIX

Calculation of Half-Power Beamwidths

```
PROGRAM BeamWidths;

(*
     This program calculates the look directions, that is, maximum
response axes (MRA's), and beamwidths at the half-power points for a
linear array of N hydrophone sensors.  It does this by solving
the equation
          SIN(NX) / N SIN(X) = 1 / SQRT(2)
for X, where
          X = Gamma0 ( SIN(Theta) - SIN(Theta0) )
and
          Gamma0 = Pi Spacing / Lambda .
'Lambda' is the design wavelength and 'Spacing' is the distance between
sensors.  'Theta0' is the MRA and 'Theta' is the half-power direction.

     Reference:  W.C. Knight, et al., "Digital Signal Processing for
                 Sonar," Proc. IEEE, Vol. 69, No. 11, 1451-1506 (1981).

     Written in Turbo Pascal (TM Borland International) Version 3.0 for
the IBM PC.
*)

CONST
  FormFeed              : CHAR        = ^l;
  Sqrt2Inv              : REAL        = 0.7071067814;

VAR
  NumElems,             (* Number of sensors *)
  NumBeams,             (* Number of beams between -Pi/2 and +Pi/2 *)
  I                                   : INTEGER;
  DeltaTheta,           (* Beamwidth at half-power points *)
  Del,                  (* Half-width in SIN(Theta)-space *)
  WidthSinTheta,        (* Full-width in SIN(Theta)-space *)
  Theta0, X0, SinTheta0, Lambda,
  Gamma0, Spacing, RadToDeg           : REAL;
  Ans                                 : CHAR;
  OutDev                              : TEXT;

FUNCTION ArcSin(   Arg  : REAL )
       : REAL;
{
     This subroutine uses a polynomial approximation given in
"Handbook of Mathematical Functions," M. Abramowitz and I.A. Stegun, eds.,
ninth printing, p. 81.  The absolute value of the error is less than 2E-8.
}

  CONST
```

```
      HalfPi            : REAL        =  1.5707963268;
      A0                : REAL        =  1.5707963050;
      A1                : REAL        = -0.2145988016;
      A2                : REAL        =  0.0889789874;
      A3                : REAL        = -0.0501743046;
      A4                : REAL        =  0.0308918810;
      A5                : REAL        = -0.0170881256;
      A6                : REAL        =  0.0066700901;
      A7                : REAL        = -0.0012624911;

  VAR
      Arc, X, X2, X3, X4, X5, X6, X7   : REAL;

  BEGIN
      X      := ABS(Arg);
      IF X > 1.0
      THEN BEGIN
           WRITELN('Argument > +/- 1 in ArcSin.');
           HALT;
           END
      ELSE BEGIN
           X2  := SQR(X);
           X3  := X*X2;
           X4  := SQR(X2);
           X5  := X*X4;
           X6  := SQR(X3);
           X7  := X*X6;
           Arc := HalfPi - SQRT(1.0-X)*( A0 + A1*X  + A2*X2
                                       + A3*X3 + A4*X4 + A5*X5
                                               + A6*X6 + A7*X7 );
           ArcSin := Arc;
           IF Arg < 0.0 THEN  ArcSin := - Arc
           END;
  END  { ArcSin };

FUNCTION Root(X0, Con : REAL) : REAL;
{
    Calculates the solution to "G(X) = Con" using the Newton-Raphson
method.  X0 is the initial guess for the root.  The calling routine
must define two functions, "F(X) = G(X)-Con" and DfDx(X), which are the
definitions of the function and its derivative.
}
CONST
  IMax = 20;
  Tolerance = 1.0E-10;

VAR
  Fx, Df, Delta, XNew, XOld        : REAL;
  I                                : INTEGER;
  Error                            : BOOLEAN;

FUNCTION F(X : REAL) : REAL;
```

```
  VAR
    N                                       : INTEGER;
    SinX, SinNX                             : REAL;

  BEGIN                                     (* F *)
    N     := NumElems;
    SinX  := SIN(X);
    SinNX := SIN(N*X);
    IF SinX <> 0.0
       THEN F := (SinNX / (N*SinX)) - Con
       ELSE F := 1.0 - Con;
  END  { F };

FUNCTION DfDx(X : REAL) : REAL;
  VAR
    N                                       : INTEGER;
    CosX, CosNX, SinX                       : REAL;

  BEGIN                                     (* DfDx *)
    N          := NumElems;
    CosX       := COS(X);
    CosNX      := COS(N*X);
    SinX       := SIN(X);
    DfDx       := (CosNX - (F(X) + Con)*CosX)/ SinX
  END  { DfDx };

BEGIN                                       (* Root *)
  Error := FALSE;
  I := 0;
  XNew := X0;
  REPEAT
    I := I+1;
    XOld := XNew;
    Fx := F(XOld);
    Df := DfDx(XOld);
    IF Df = 0.0 THEN BEGIN
      Error := TRUE;
      WRITELN(CHR(7),'ERROR:  Denominator (derivative) is 0.');
      END  { Error }
    ELSE BEGIN
      Delta := Fx/Df;
      XNew := XOld - Delta;
      END { New Root };
  UNTIL Error
    OR  (I > IMax)
    OR  (ABS(Fx) < Tolerance)
    OR  (ABS(Delta) < Tolerance*ABS(XNew));
  Root := XNew;


  IF I > IMax THEN BEGIN
```

```
    WRITELN(CHR(7),'ERROR:  Failed to converge in ',IMax,' iterations.');
    Error := TRUE
    END  { Failed convergence };

END  { Root };


BEGIN                                    (* ExactBeamWidths *)
  Ans := 'n';
  WRITE('Send results to printer (Y/N)? '); READLN(Ans);
  IF (Ans = 'y') OR (Ans = 'Y')
     THEN ASSIGN(OutDev, 'LST:')
     ELSE ASSIGN(OutDev, 'CON:');
  WRITE('How many sensors? '); READLN(NumElems);
  WRITE('What is the wavelength? '); READLN(Lambda);
  WRITE('What is their spacing? '); READLN(Spacing);
  RadToDeg := 180./Pi;
  Gamma0 := Pi*Spacing/Lambda;
  Theta0 := 0.;
  SinTheta0 := 0.;
  I := 0;
  X0       := 0.443*Pi / NumElems;          (* Approximate half-power width.
*)
  X0       := Root( X0, Sqrt2Inv );              (*  Exact  "     "     "
*)
  Del           := X0 / Gamma0;
  WidthSinTheta := 2*Del;
  DeltaTheta    := 2*ArcSin( Del );
  NumBeams      := 2*TRUNC(0.5/Del) + 1;
                                           (*   Print results.    *)
  WRITELN(OutDev, 'Number of sensors = ', NumElems);
  WRITELN(OutDev, 'Wavelength        = ', Lambda:8:5);
  WRITELN(OutDev, 'Spacing           = ', Spacing:8:5);
  WRITELN(OutDev, 'Maximum Response Axis spacing');
  WRITELN(OutDev, 'in Sin(Theta)-space is ',
                   WidthSinTheta:11:9,'.');
  WRITELN(OutDev, 'Number of beams is ', NumBeams, '.');
  WRITELN(OutDev);
  WRITELN(OutDev);
  WRITELN(OutDev,'Num.   Theta0    DelTheta   ');
  WRITELN(OutDev);
  WRITELN(OutDev, I:3, RadToDeg*Theta0:11:5, RadToDeg*DeltaTheta:11:5);
  I := I + 1;

  WHILE I <= NumBeams DIV 2
  DO BEGIN
     (*   Find the direction of the next beam.    *)
     SinTheta0  := SinTheta0 + WidthSinTheta;
     Theta0     := ArcSin( SinTheta0 );
     IF ABS( SinTheta0 + Del ) <= 1.0
        THEN DeltaTheta :=   ArcSin( SinTheta0 + Del )
                           - ArcSin( SinTheta0 - Del )
```

```
        ELSE DeltaTheta := 0.0;

      (*   Print results.   *)
      WRITELN(OutDev, I:3, RadToDeg*Theta0:11:5, RadToDeg*DeltaTheta:11:5);
      I          := I+1
      END;

  WRITELN(OutDev, FormFeed);
END  { BeamWidths }.
```

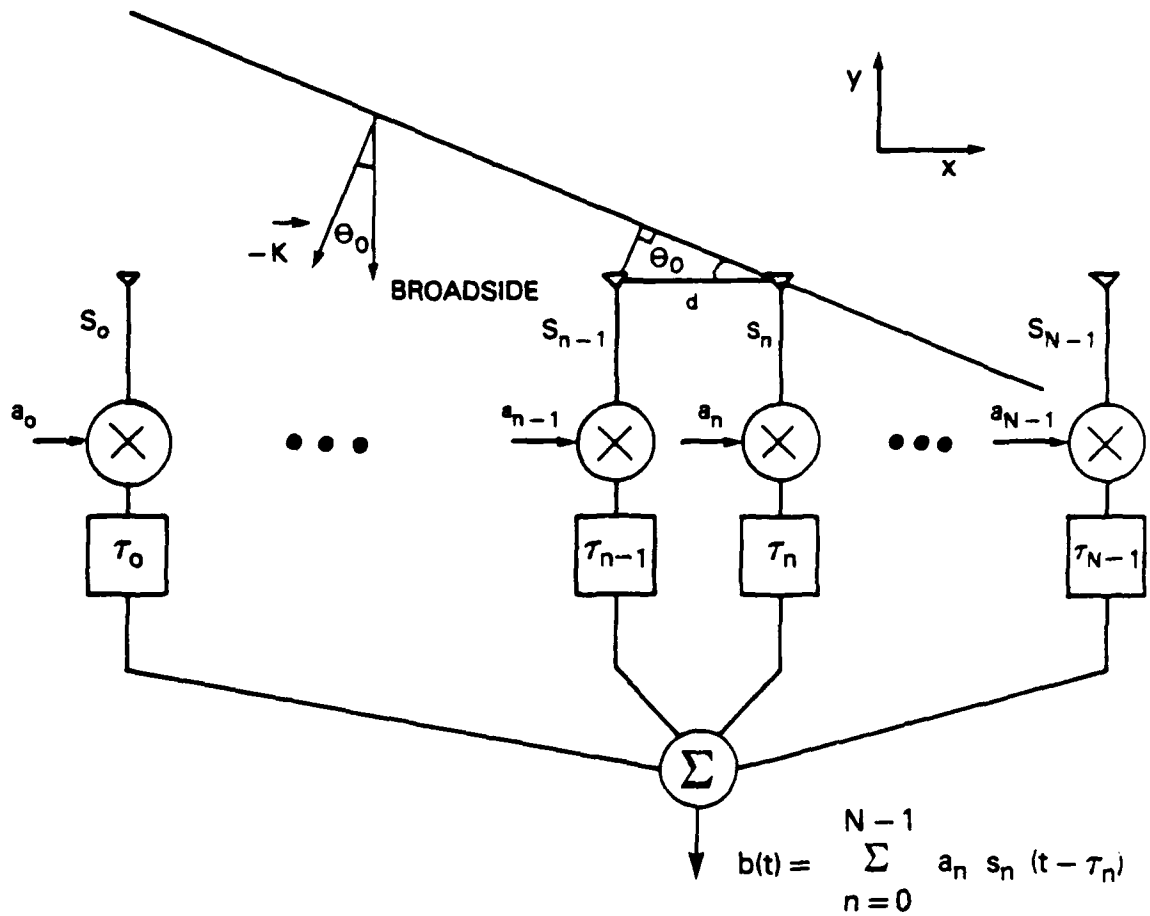

Figure 1. N-sensor linear beamformer.

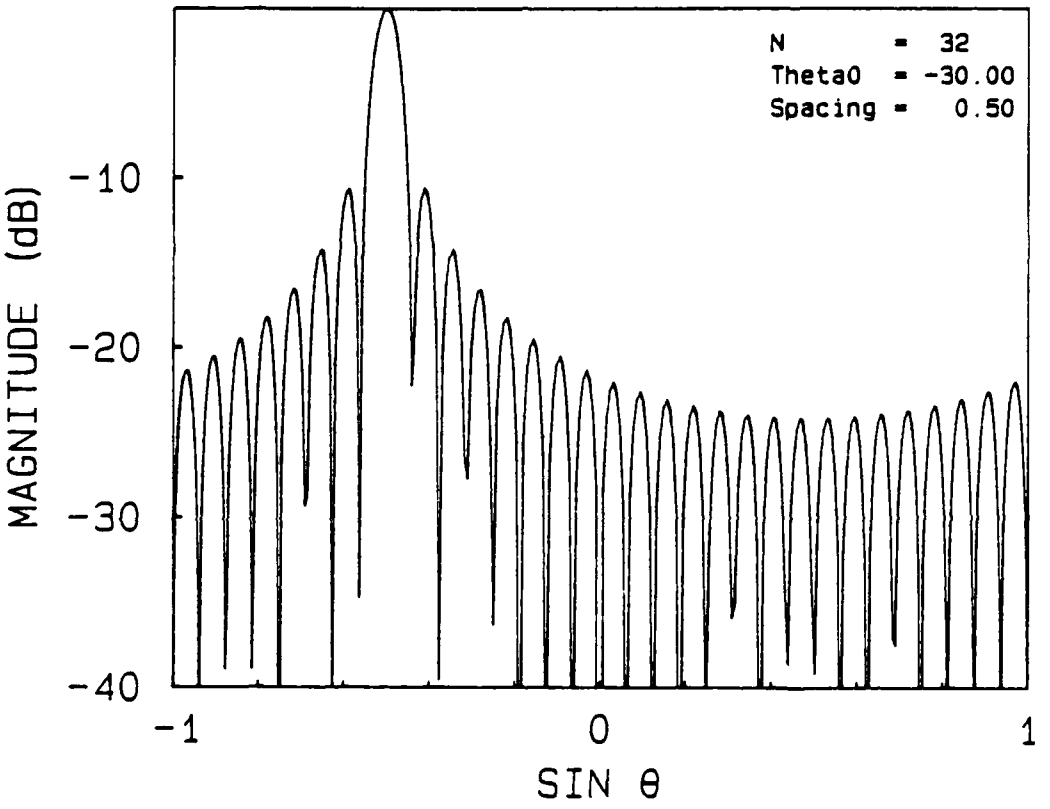

Figure 2. Array response pattern.

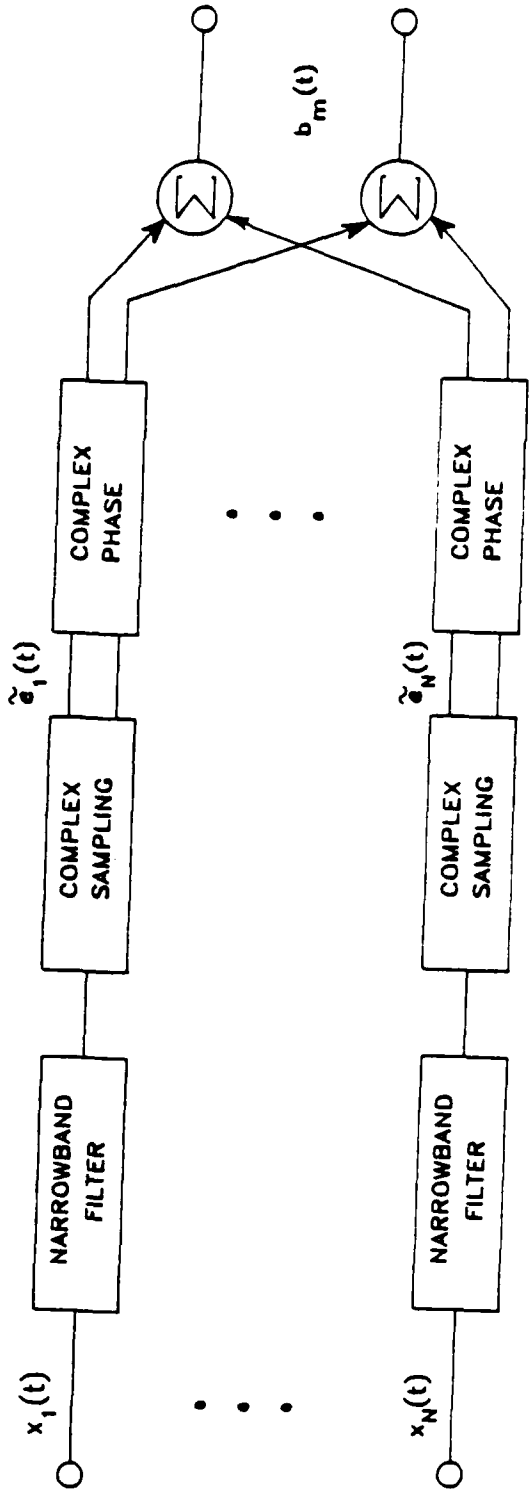

Figure 3. Phase-shift beamforming.

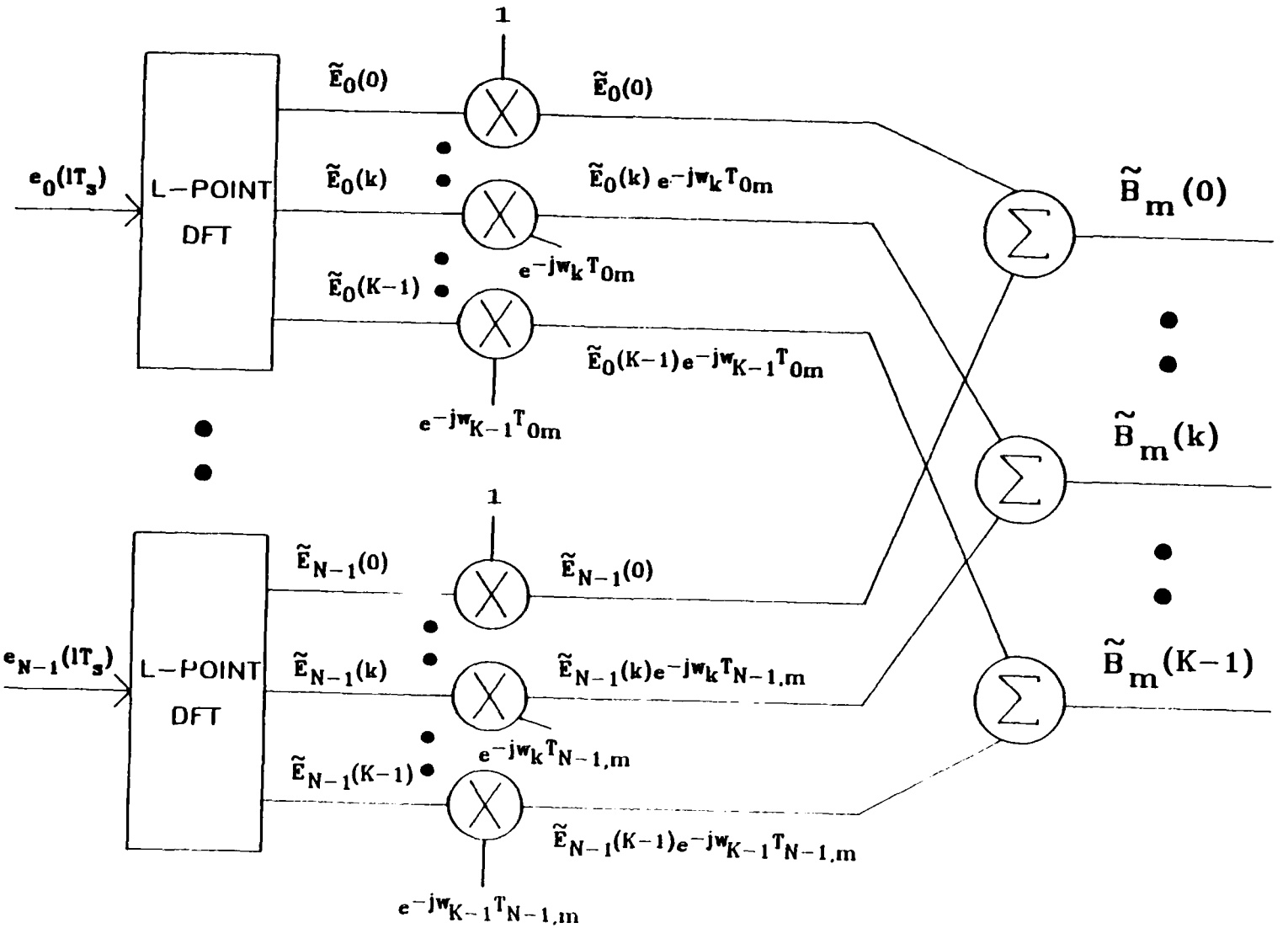

Figure 4. Fourier transform beamforming.

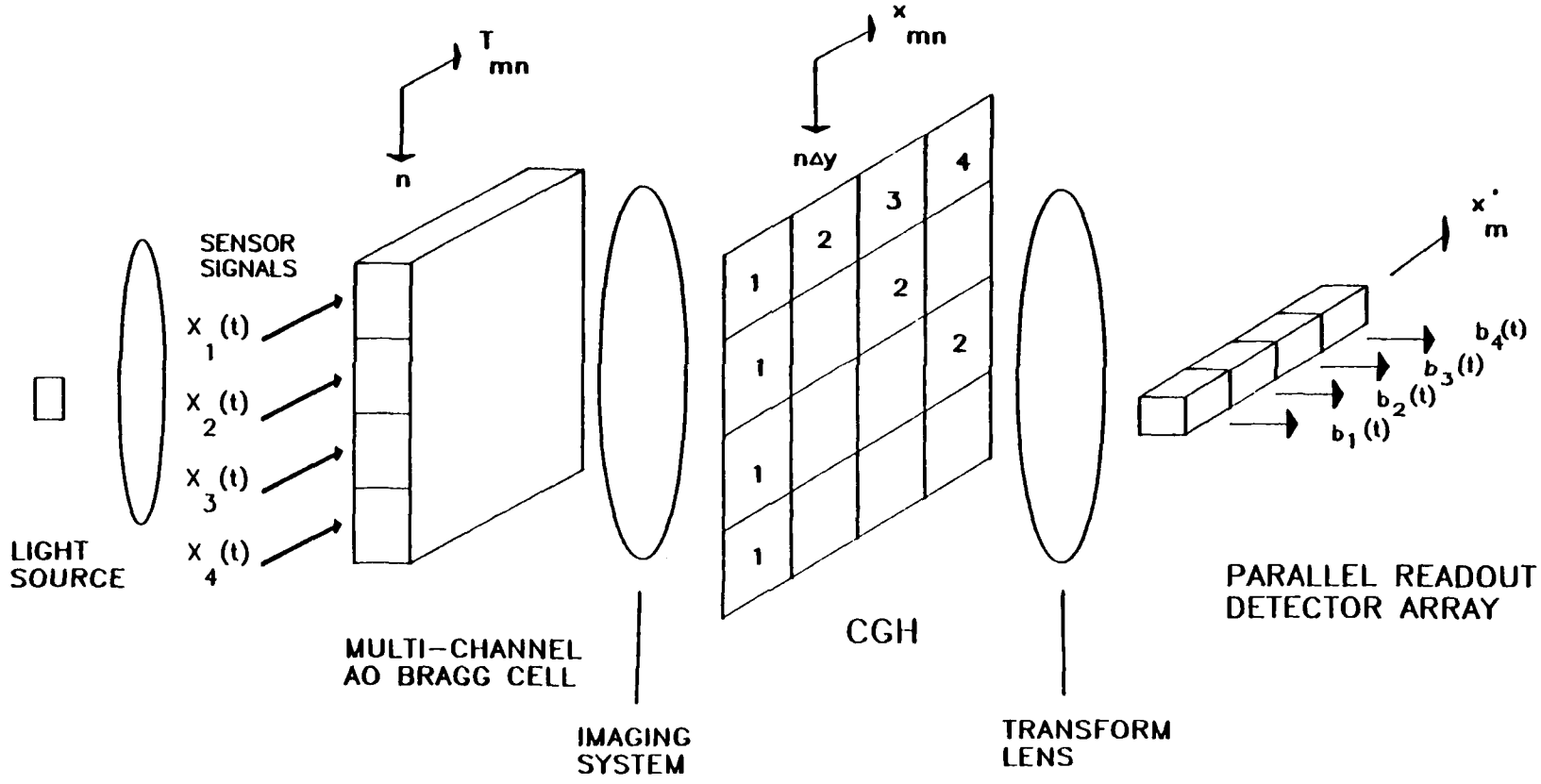

Figure 5. Space-integrating optical beamformer.

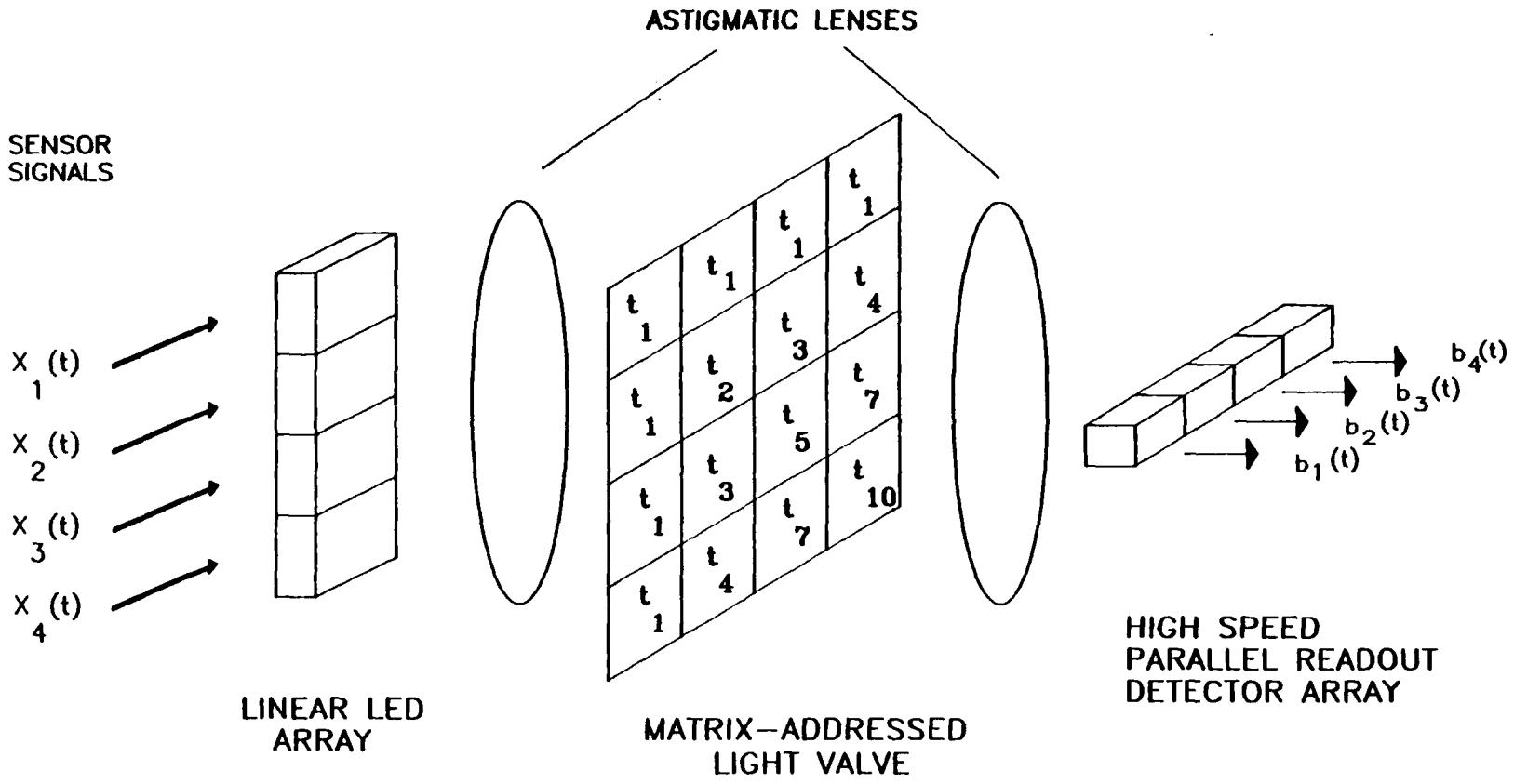

Figure 6. Delay-sum optical beamformer.

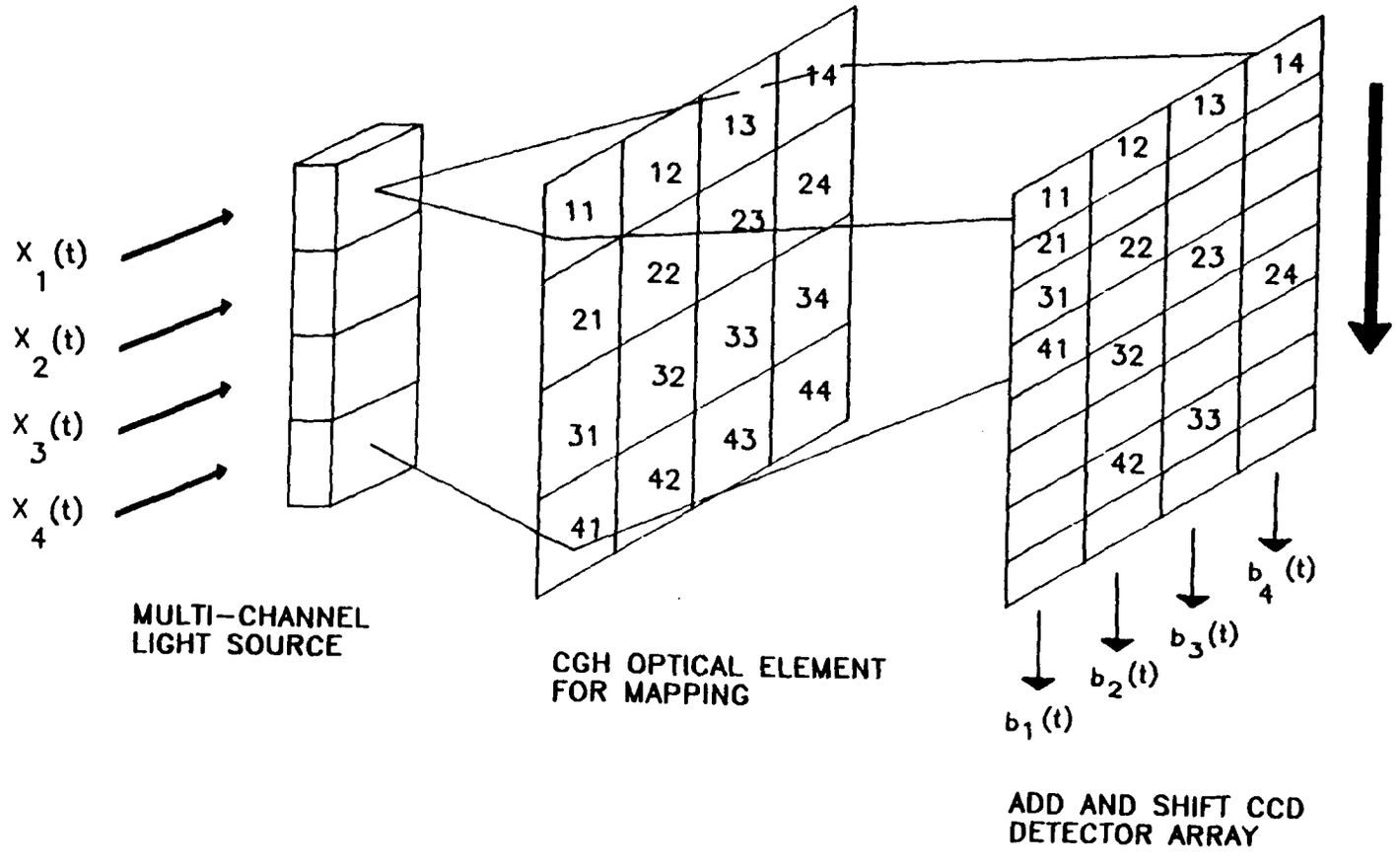

Figure 7. Sum-delay optical beamformer.

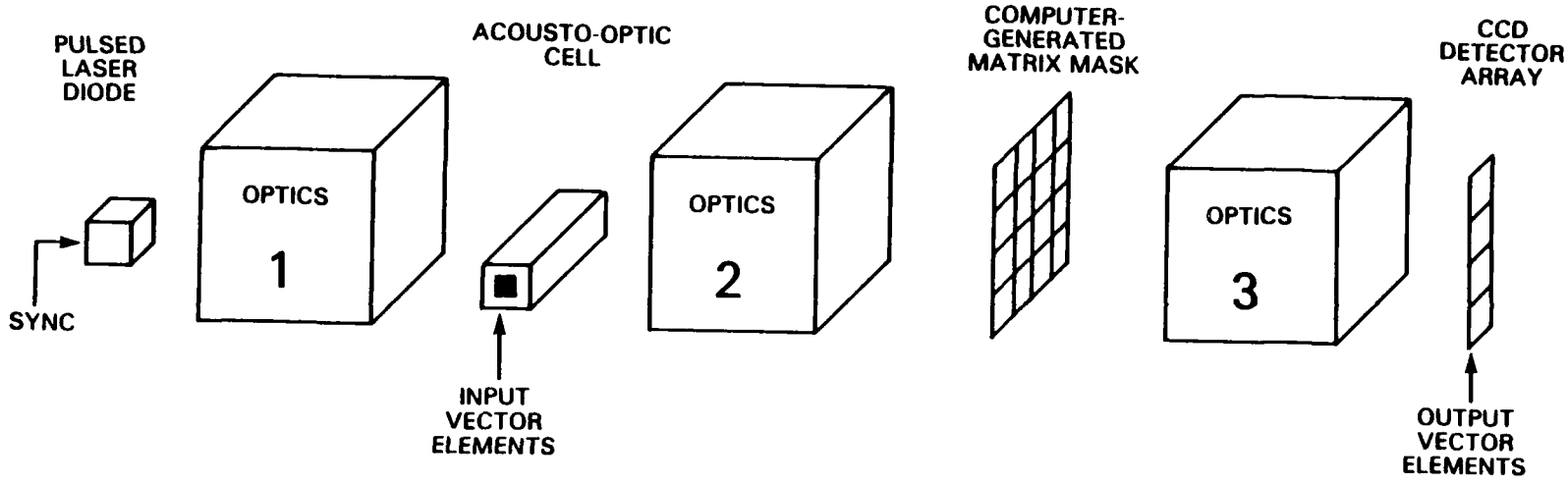

Figure 8. Frequency-domain vector-matrix multiplication beamformer.

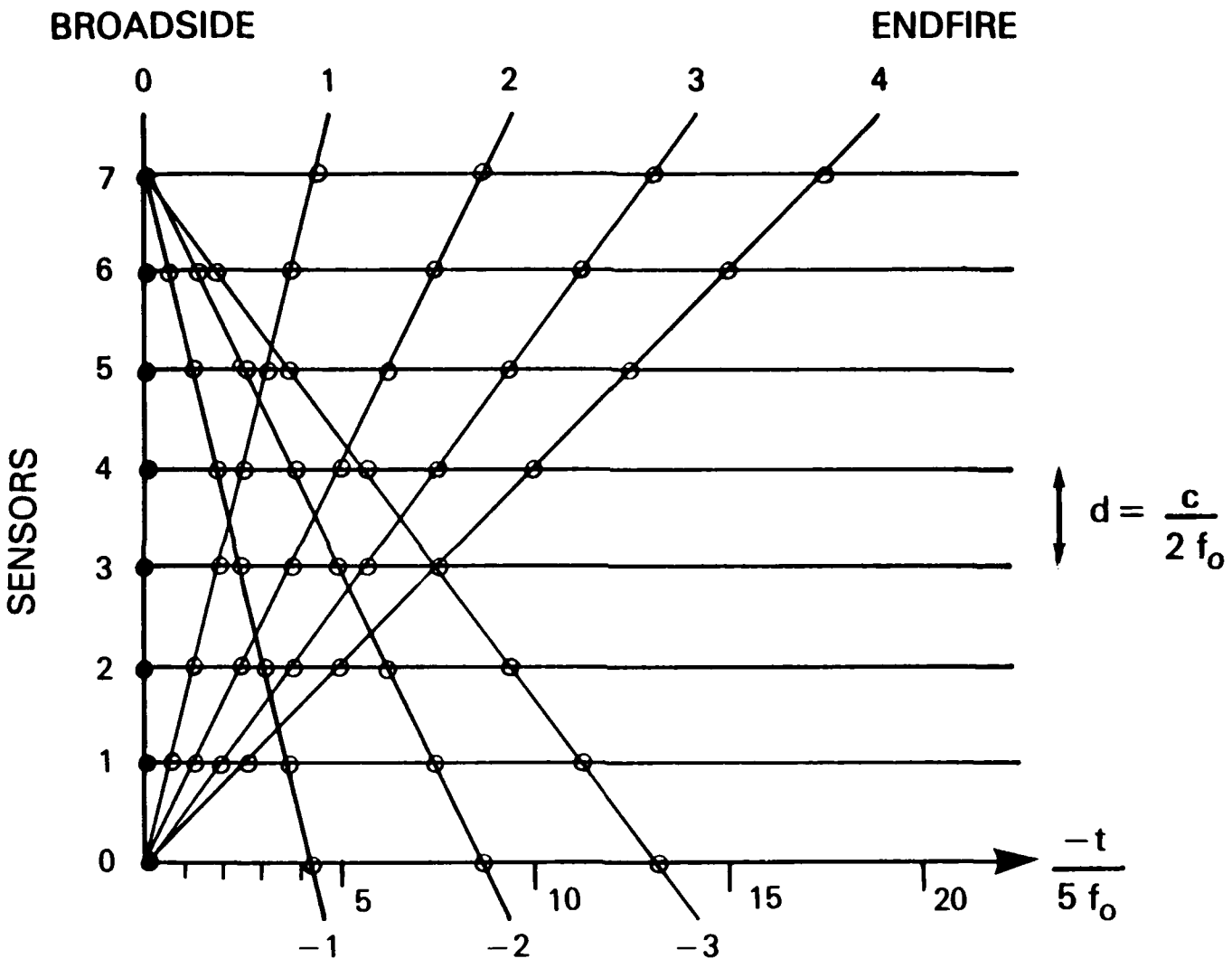

Figure 9. Depiction of beamforming operation as a set of tapped delay lines.

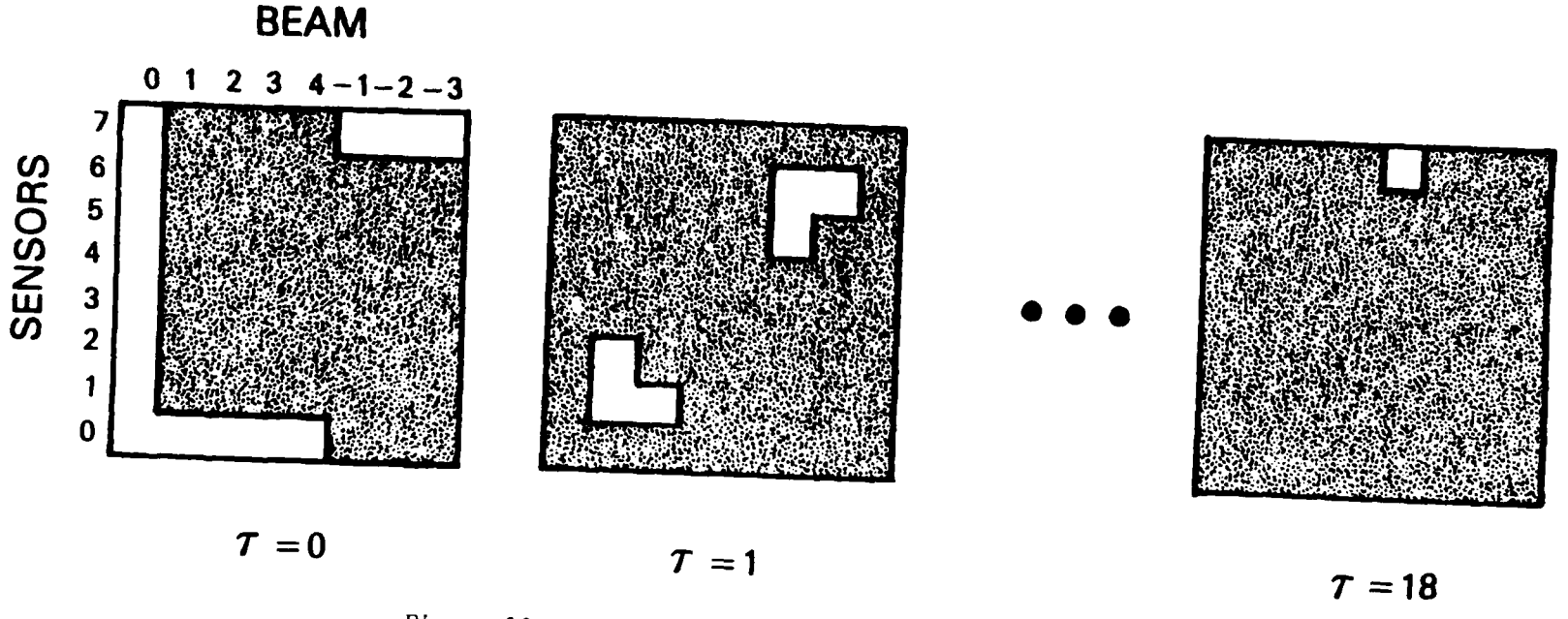

Figure 10. Three of the masks defined by Table 1.

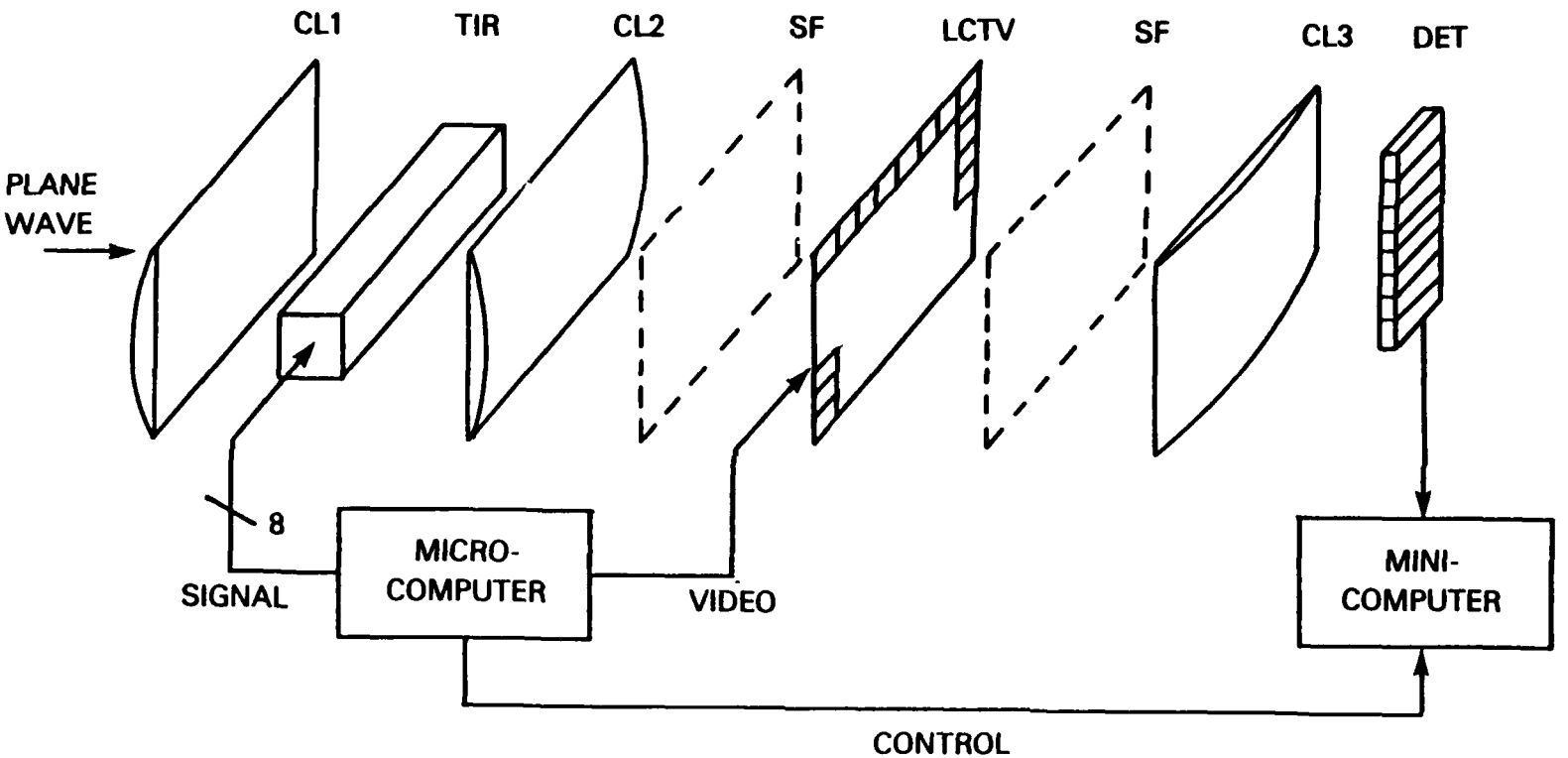

Figure 11. Experimental layout. CL1-3 are cylinder lenses. SF - spatial filter (optical details not shown). TIR - electro-optic total-internal-reflection modulator. LCTV - liquid crystal television with the mask for t = 0 shown. DET - photodiode detector array.

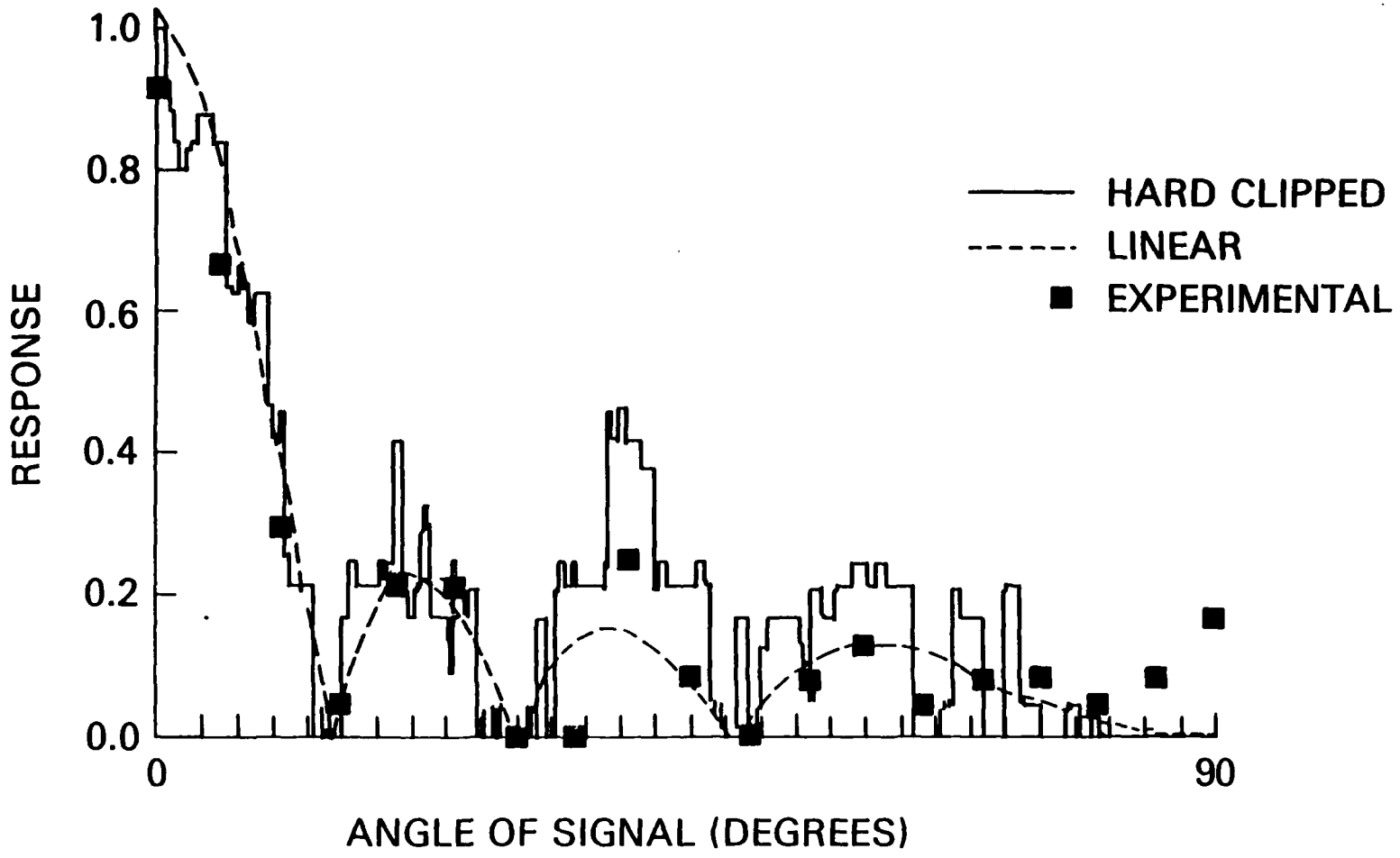

Figure 12. Response of broadside beam (0) for linear and hardclipped beamformers, and experimental results.

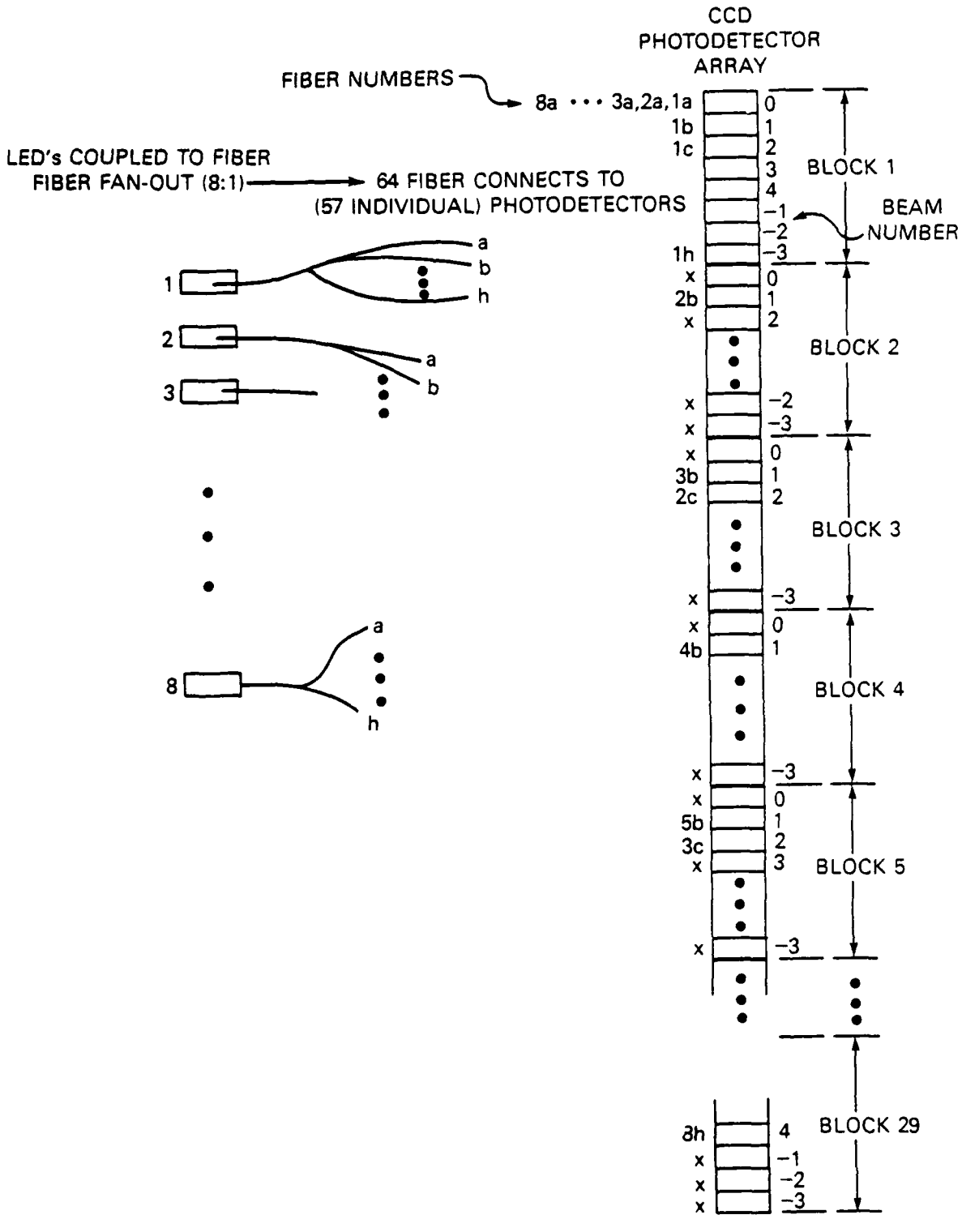

Figure 13. Fiber-optic/CCD beamformer.

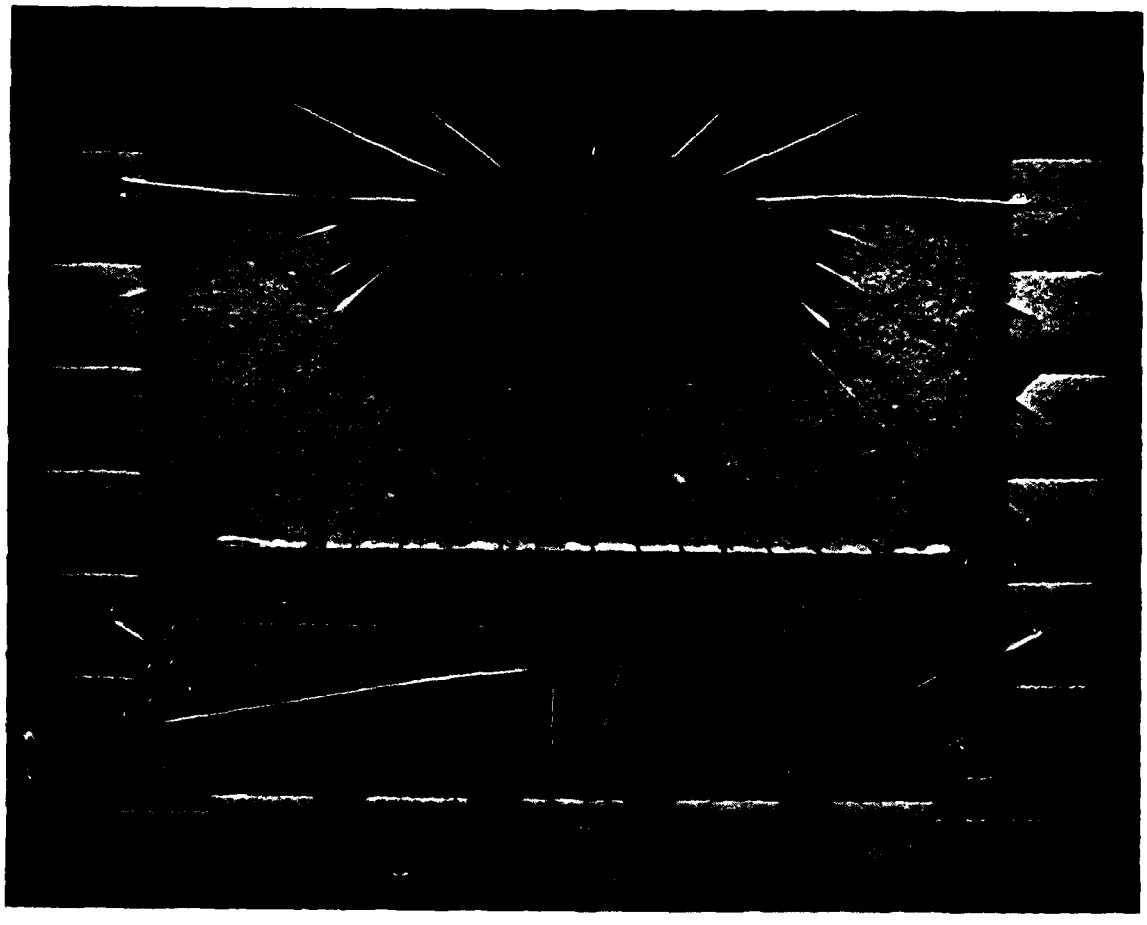

Figure 14. Photodetector/CCD MUX chips.

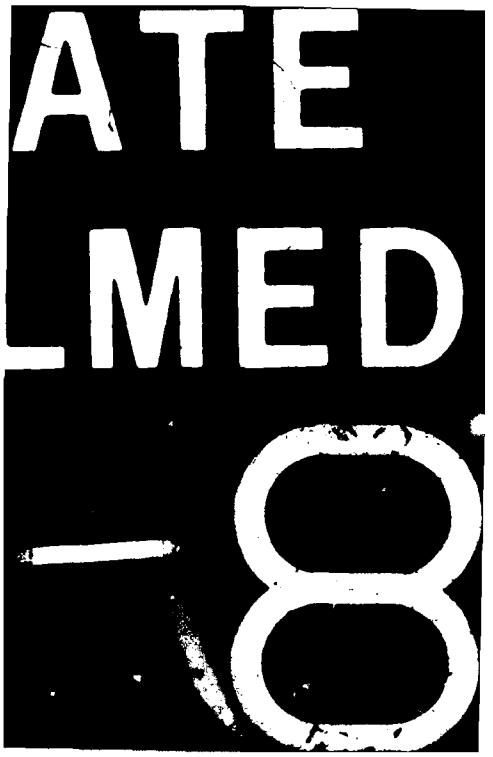
ATE
LMED
8